Integrated Longitudinal and Lateral Tire/Road Friction Modeling and Monitoring for Vehicle Motion Control

Li Li, *Member, IEEE*, Fei-Yue Wang, *Fellow, IEEE*, and Qunzhi Zhou

***Abstract*—A proper tire friction model is essential to model overall vehicle dynamics for simulation, analysis, or control purposes since a ground vehicle's motion is primarily determined by the friction forces transferred from roads via tires. Motivated by the developments of high-performance antilock brake systems (ABSs), traction control, and steering systems, significant research efforts had been put into tire/road friction modeling during the past 40 years. In this paper, a review of recent developments and trends in this area is presented, with attempts to provide a broad perspective of the initiatives and multidisciplinary techniques for related research. Different longitudinal, lateral, and integrated tire/road friction models are examined. The associated friction-situation monitoring and control synthesis are discussed with a special emphasis on ABS design.**

***Index Terms*—Antilock brake systems (ABSs), steering control, tire/road friction identification, tire/road friction modeling.**

I. Introduction

INCREASING requirements on ride safety and comfort inspired the concepts of intelligent vehicles (IVs) more than 20 years ago [1]–[3]. Serving as one important part of IV research, tire/road friction modeling, online monitoring, and advanced vehicle control systems have gained significant interests worldwide [4]–[11], [125]–[127].

Friction force at the tire/road interface is the main mechanism for converting motor torque to longitudinal force, and is tightly related to vehicle steering too. Analysis of tire/road friction can provide us an insight into the understanding of vehicle dynamics so as to improve ride performance [8]–[11]. Therefore, it attracted continuous efforts in the last four decades.

The main task of tire/road friction modeling and monitoring is to determine the relationship between friction forces and longitudinal/lateral slip ratios. However, tire/road friction phenomenon is hard to analyze especially for the following three reasons.

First, friction force is affected by several different factors including tire/road-surface conditions, tire pressure, vehicle load, and steering angle, etc. It is believed to come from three major aspects: deformation, adhesion, and tearing/wear [4]–[9]. The movement of a tire slider on rough surfaces results in the deformation of rubber called asperities. The load of a vehicle causes these asperities to penetrate the rubber. When the rubber drapes over these asperities, it yields a resistance force. Deformation friction provides most of the friction force, especially when the road is wet. Adhesion is a property of the rubber that causes it to stick to other materials. It appears to come from two factors: one is related to the molecular bonds between tread rubber and road; the other lies in the shearing of the rubber just below the surface layer. The nature of the first factor is not completely clarified [4]–[7]. However, it is believed that these forces are highly dependent on sliding velocity and tire surface temperature. In addition to adhesive friction and deformation friction, the rubber produces traction forces by means of tearing and wear too. An appropriate tire model should be able to represent the different effects of all these factors.

Second, the nonlinear and dynamic properties of tire/road friction, e.g., the viscous and hysteresis phenomena, are difficult to analytically describe, while most empirical tire/road friction formulas are hard to explain by physical laws. Therefore, applications require a manageable tire model, in which measurement data could be translated sensibly into tire properties and vice versa.

Third, an appropriate tire/road friction model should be easy to employ in vehicle control systems, e.g., antilock brake systems (ABSs) [8]–[11]. It should be able to express specific vehicle driving behaviors in terms of tire characteristic parameters, which finally contributes to the desired tire properties that are given to tire manufacturers and vehicle designers.

In order to overcome these difficulties and improve driving performance, numerous tire friction models had been proposed, as well as related monitoring and control synthesis. By scanning the previous research efforts, this paper sequentially looks into the following topics: 1) longitudinal tire/road friction modeling; 2) lateral tire/road friction modeling; 3) integrated tire/road friction modeling; 4) tire/road friction monitoring and control synthesis; and 5) ABSs design.

This overview of these diverse issues aims to provide useful perspectives for researchers who are involved in this field.

Manuscript received January 16, 2005; revised July 21, 2005. This work was supported in part by the Federal Department of Transportation through the Advanced Traffic and Logistics Algorithms and Systems (ATLAS) Research Center at the University of Arizona and Grants 60125310, 60334020, 2002CB312200, 2004AA1Z2360, and 2004GG1104001 from China. The Associate Editor for this paper was M. Papageorgious.

L. Li is with Department of Systems and Industrial Engineering, University of Arizona, Tucson, AZ 85719 USA (e-mail: li1@email.arizona.edu).

F.-Y. Wang is with the Key Laboratory for Complex Systems and Intelligence Science, Chinese Academy of Sciences, Beijing, China, and with the Program in Advanced Research for Complex Systems, Department of Systems and Industrial Engineering, University of Arizona, Tucson, AZ 85719 USA (e-mail: feiyue@sie.arizona.edu).

Q. Zhou is with the Key Laboratory for Complex Systems and Intelligence Science, Chinese Academy of Sciences, Beijing 100080, China (e-mail: zhouqunzhi@cas-ic.com).

Digital Object Identifier 10.1109/TITS.2005.858624

Although it is impossible to cover hundreds of publications in this area, the key findings and trends of research are included. The focus is on recent literature, since good reviews already exist on the relatively long history of the subject [8], [10], [21], [35], [46], [103]–[105], [121].

II. Longitudinal Tire/Road Friction Modeling

A. Longitudinal Tire/Road Friction Characteristics

Literatures for longitudinal tire/road friction modeling could be dated back to the late 1980s and early 1990s [12]–[15]. In most proposed models, the friction force is assumed to be determined by wheel slip with regard to some other parameters.

Let us use F_x to denote longitudinal friction force and F_z to denote the normalized force. The longitudinal tire/road friction coefficient could be defined as

$$\mu_x = \frac{F_x}{F_z}. \tag{1}$$

The longitudinal wheel slip s_x can be defined as

$$s_x = \begin{cases} 1 - \frac{R\omega}{v_x}, & \text{if } v_x > R\omega, v \neq 0, \text{ braking} \\ 1 - \frac{v_x}{R\omega}, & \text{if } v_x < R\omega, \omega \neq 0, \text{ driving} \end{cases} \tag{2}$$

where R is the effective radius of the wheel, ω represents the angular velocity, and v_x represents the longitudinal velocity.

The two plots in Fig. 1, which are obtained by Harned *et al.* [12], demonstrate the typical variation trends between μ_x and s_x under different road conditions [Fig. 1(a)], or different vehicle velocities [Fig. 1(b)]. Normally, μ_x increases when vehicle velocity decreases or the road surface becomes rougher.

As shown in Fig. 2, with given conditions, μ_x is a nonlinear function of s_x with a distinct maximum (maximum of friction $\mu_{x,\max}$, 1 in Fig. 2). The variation relationship of μ_x and s can be clearly distinguished into two parts: the steady rising part of the μ_x–s_x graph (3 in Fig. 2) and the local sliding part in which μ_x gradually decreases to $\mu_{x,\text{glide}}$ (2 in Fig. 2). Usually, $\mu_{x,\text{glide}}$ is notably smaller than $\mu_{x,\max}$.

B. Some Longitudinal Tire/Road Friction Models

From the theoretical aspects, different longitudinal tire/road friction models can be classified into two types: empirical (semiempirical) models and analytical models. The empirical (semiempirical) models are based on curve-fitting techniques, which usually formulate the μ_x–s_x curve into a complex function of μ_x mainly in terms of s_x.

Empirical (semiempirical) models can accurately catch the steady-state characteristics of tire/road friction phenomena [13]–[15]. However, they cannot describe several significant dynamic behaviors such as hysteresis. That is why they were also called static models in some literatures. Moreover, they lack physical interpretations, and cannot directly reflect the effects of some special factors such as humidity of the road or tire pressure. Thus, some analytical models, especially the brush model in [16], [17], and [22]–[37], became popular recently.

Most analytical models use differential equations to describe tire/road friction properties. For instance, the main idea of the brush model is to view the tire as a collection of elastic bristles that touches the road plane and deflects in the direction parallel to the road surface. The bristles' compliance is added into a set of forces and torques acting on the tire, which finally leads to a set of differential equations. It has been proven that the brush model can be used to interpret dynamic tire/road phenomena. Therefore, it is also called dynamic model in some literatures.

Constrained by the length, this paper only discusses some representative longitudinal tire/road friction models as below (Table I).

1) Piecewise Linear Model: This is a very simple model, where the μ_x–s_x relationship is roughly approximated with a piecewise linear function that passes the original point, $\mu_{x,\max}$, and $\mu_{x,\text{glide}}$ (see Fig. 2).

Although it cannot accurately capture the nonlinear dynamic characteristics of tire/road friction, this model still received considerable attention due to its simplicity. A typical usage of this model will be discussed in Section VI-A.

2) Burckhardt Model: It is a frequently mentioned tire/road friction model that was proposed in [18]. Originally, it was written as

$$\mu_x = \left(C_1\left(1 - \mathrm{e}^{-C_2|s_x|}\right) - C_3|s_x|\right)\mathrm{e}^{-C_4 v_x} \tag{3}$$

where C_i, $i = 1, \ldots, 4$, are parameters that can be determined by experimental data. The item $\mathrm{e}^{-C_4 v_x}$ was added to model the difference of friction under high and low speeds.

It was shown that this model can approximately describe the μ_x–s_x curve with properly assigned C_i. However, because of nonlinearity, its parameter-identification cost is relatively high. Thus, several revised formulas from (3) were proposed. For example, it was modified in [19] as

$$\mu_x = C_1\mathrm{e}^{-C_2|s_x|} \cdot |s_x|^{(C_3|s_x|+C_4)} \cdot \mathrm{e}^{-C_5 v_x} \tag{4}$$

of which the logarithm linear formation can be written as

$$\ln \mu_x = C_1 - C_2|s_x| + (C_3|s_x| + C_4) \cdot \ln|s_x| - C_5 v_x. \tag{5}$$

It is clear that model (5) is much simpler to identify than the original model, and has similar approximation properties.

3) Rill Model: The Rill model proposed in [20] is another semiempirical model. It is based on steady-state force/torque characteristics of a tire together with a simple transient tire deflection model. It calculates the slip in steady state and a corresponding tire force with a curve fit using initial inclination at $s_x = 0$ and location/magnitude of $\mu_{x,\max}$ and $\mu_{x,\text{glide}}$ as parameters. The nonlinear dependence of the vertical load is handled by an interpolation between a set of the parameters for predefined-load cases.

4) Magic Formula: In 1980, Pacejka, in conjunction with Volvo, developed an empirical formula in which the properties shown above could be described in closed form [13]–[15]. It was originally written as

$$\mu_x = C_1 \sin\left(C_2 \tan^{-1}\left(C_3 s_x - C_4\left(C_3 s_x - \tan^{-1}(C_3 s_x)\right)\right)\right) \tag{6}$$

where C_i, $i = 1, \ldots, 4$, are determined by experiments.

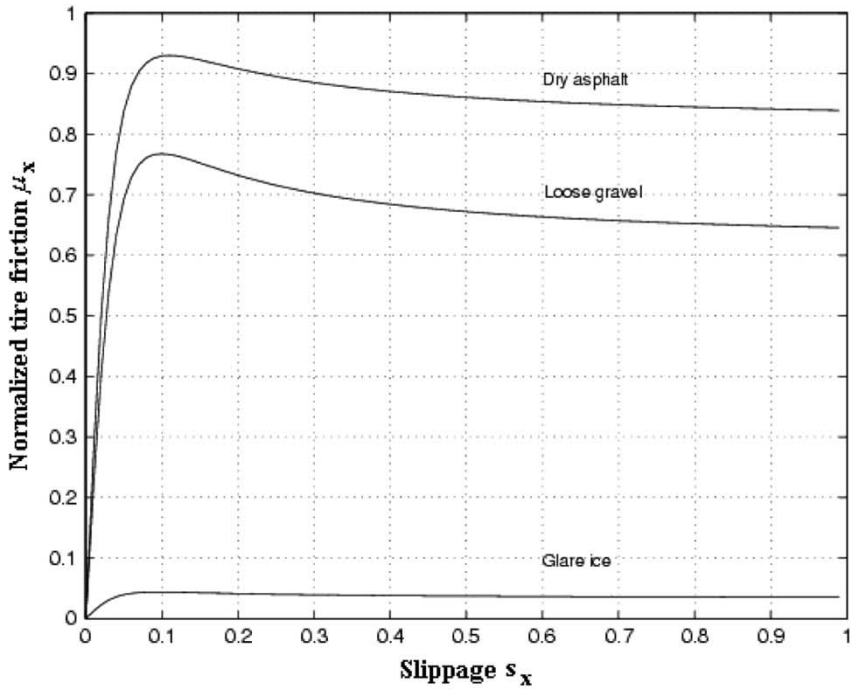

(a)

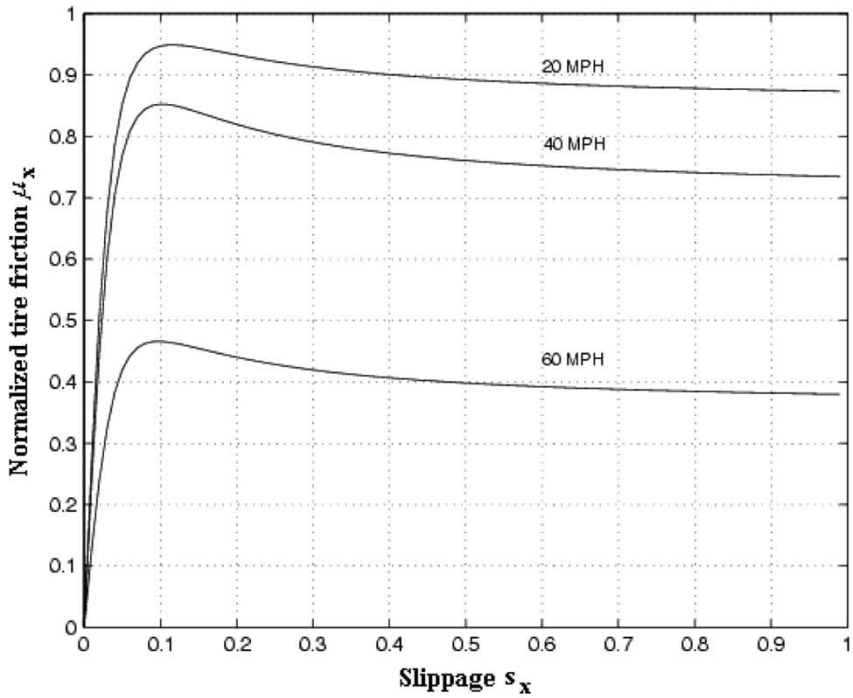

(b)

Fig. 1. Typical tire/road friction profiles for (a) vehicle running on different road-surface conditions with velocity 20 mi/h; (b) vehicle running on dry asphalt road with varied velocities [12].

This model received successive modifications in the last two decades and has now become the most important semiempirical tire friction model. It can now be applied to denote aspects such as camber, vertical load, and transient behaviors. The level of details is controlled by user modes (UMs) specified in Table II.

This "magic formula" had been widely used in tire/road friction simulation and control-system design [13]–[15], [21], [109], [110]. However, it is overparameterized and thus, difficult to analyze. That is partially why the above model is called "magic formula."

5) Dahl Model: Dahl developed a comparatively simple tire/road friction model in the 1970s, which is indeed a generalization of Coulomb friction. However, this model can produce a smooth transition around zero velocity. The frictional hysteresis during presliding is approximated by a generalized first-order

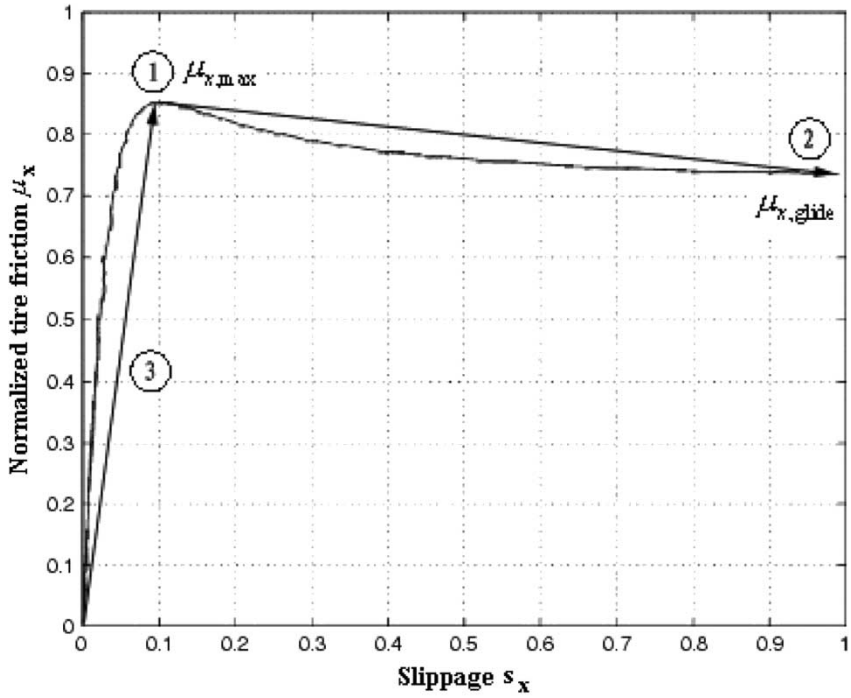

Fig. 2. Diagram of steady friction and sliding.

TABLE I
SOME REPRESENTATIVE LONGITUDINAL TIRE/ROAD FRICTION MODELS

User Model	Meanings
	steady state user modes
UM0	only vertical spring
UM1	pure longitudinal slip
UM2	pure lateral slip
UM3	longitudinal and lateral slip (not combined)
UM4	combined slip forces, steady state
	transient user modes
UM11	pure longitudinal slip
UM12	pure lateral slip
UM13	longitudinal and lateral slip (not combined)
UM14	combined slip forces

equation of the position depending only on the sign of the velocity [22], [23].

Specifically, Dahl proposed the following equation

$$\frac{dF}{dt} = \sigma_0 \left(1 - \text{sgn}(v_r) \cdot \frac{F}{F_\text{s}}\right)^{\delta_\text{d}} v_\text{r} \tag{7}$$

where σ_0 denotes the initial stiffness of the contact at velocity reversal, δ_d denotes a model parameter determining the shape of the hysteresis, and v_r is the relative moving speed.

The Dahl model captures many important phenomena of friction including zero slip displacement and hysteresis. The most instructive contribution of Dahl is that he modeled the stress–strain curve by a differential equation. However, the Dahl model has to be improved in several aspects. For example, it does not describe the relationship between the velocity and the friction, and it neglects the stiction. Thus, Dahl's dynamic-modeling idea soon led to the birth of several other models, such as the Bliman–Sorine model [24]–[26] and the LuGre model.

6) LuGre Model: Inspired by the technique used in the Dahl model, Canudas de Wit *et al.* proposed a new model that incorporated the idea of introducing an averaged characteristic presliding displacement [27], [28]. Since this model was developed at the universities of Lund and Grenoble, it is then called the LuGre model.

The LuGre model combines the merits of the Dahl model with several other steady-state characteristics, e.g., the Stribeck curve. However, the interpretation of the internal state has been set upon the bristle model instead of the average random behavior model of the asperities. From this viewpoint, tire surfaces are considered to be very irregular at the microscopic level and two surfaces, therefore, make contact at a number of asperities. When tangential force is applied, the bristles will deflect like springs, which gives rise to the friction force [see Fig. 3(a)].

By defining a variable z to represent the average deflection of the asperities as shown in Fig. 3(b), the LuGre model for the tire/road friction model can be formulated as

$$\begin{cases} \frac{dz}{dt} = v_\text{r} - \sigma_0 \frac{|v_\text{r}|}{g(v_\text{r})} z \\ v_\text{r} = v_x - r\omega \\ F_x = \left(\sigma_0 z + \sigma_1 \frac{dz}{dt} + \sigma_2 v_\text{r}\right) F_z \end{cases} \tag{8}$$

where σ_0 is the stiffness, σ_1 is a damping coefficient, and σ_2 is a proportional coefficient to the relative velocity to account for viscous friction.

The function $g(\cdot)$ is positive and depends on many factors such as material properties and temperature. For typical bearing

TABLE II
SPECIFICATION OF THE MAGIC FORMULA UMS

Year	Model Name	Model Properties	Features
	Piecewise Linear Model	Empirical	1. Cannot accurately fit curves 2. Easy to identify
1993	Burckhardt Model	Semi-Empirical	1. Can accurately fit curves 2. Has some revised formula
1994	Rill Model	Semi-Empirical	Easy to identify
1987	Magic Formula	Semi-Empirical	1. Can accurately fit curves 2. Has lost of revised formula 3. Can employ different factors
1977	Dahl Model	Analytical	1. Can describe Coulomb friction. 2. Can produces smooth transition around zero velocity
1991	Bliman-Sorine Model	Analytical	Can capture the Stribeck effect in addition to Dahl model
1995	LuGre Model	Analytical	Can combine pre-sliding & sliding in addition to Bliman-Sorine Model

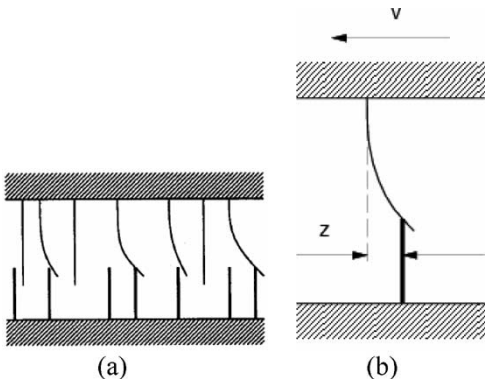

Fig. 3. Bristle model. (a) Friction interface between two surfaces is thought of as a contact between bristles. For simplicity, the bristles on the lower part are shown as being rigid; (b) average deflection of the asperities [27].

friction, $g(v)$ will decrease monotonically from $g(v(t=0))$ so as to model the Stribeck effect when v increases. Usually, it is written as $g(v_{\rm r}) = \mu_{\rm c} + (\mu_x - \mu_{\rm c}){\rm e}^{-|v_{\rm r}/v_{\rm s}|^{1/2}}$, where $\mu_{\rm c}$ is the normalized Coulomb friction and $v_{\rm s}$ is the Stribeck relative velocity. Normally, it is assumed that $\mu_{\rm c} \leq \mu_{\rm s} \in [0, 1]$.

Since the LuGre model is still a first-order model, it is easier to analyze than most second-order models. Its properties had been well explored in [27]–[38], of which the most important two are that the deflection z should be finite and the system (8) is dissipative. Deur and Canudas de Wit *et al.* independently showed that the LuGre model can be physically explained using distributed tire models in [33]–[37]. In [92], it is further shown that a slightly modified LuGre model can incorporate disturbance caused by unsteady road surfaces and other reasons. Because of its simplicity and convenient combination of presliding and sliding into one equation set, the LuGre model has become a popular model for friction compensation and estimation after its initial presentation.

III. LATERAL TIRE/ROAD FRICTION MODELING

A. Some Lateral Tire/Road Friction Models

Lateral vehicle dynamics has been studied since the 1950s [39], [40]. It is found that for a given tire/road friction condition and a constant load, lateral tire force will initially increase with slip angle and then saturate (see Fig. 4).

In the last two decades, some friction models were proposed to handle lateral tire/road friction independently of longitudinal friction. This kind of methods greatly simplifies the steering-controller design problems.

Let us discuss the front-steering vehicle for instance. Supposing that the vehicle is moving on a flat road surface, the external front-steering model can be formulated as shown in Fig. 5 [40]–[42].

Here, the reference point CG is chosen to represent the center of gravity for the vehicle body, where vehicle velocity v is defined. Symbols A and B denote the positions of the front and rear tire/road interfaces, respectively. The heading angle ψ is the angle from the guideline to the longitudinal axis of vehicle body AB. The slide slip angle β is the angle from the longitudinal axis of the vehicle body to the direction of the vehicle velocity. $\delta_{\rm f}$ is the front-tire steering angle and $\delta_{\rm r}$ is the rear-tire steering angle. Yaw rate is denoted as r. $f_{\rm f}$ and $f_{\rm r}$ are the front and rear tire forces that are perpendicular to the directions of tire movements, respectively. $f_{\rm w}$ is the wind force acting on the aerodynamic center of the side surface and $l_{\rm w}$ denotes the distance between CG and the aerodynamic center of the side surface. $l_{\rm fs}$ and $l_{\rm rs}$ denote the distances from the front and rear sensor "looking at" points to CG, respectively. $y_{\rm f}$ and $y_{\rm r}$ represent the displacements from the front and rear "looking at" points to the guideline. Other variables are given in Table III, in which the values are set for a city bus O 305 based on an International Federation of Automatic Control (IFAC) benchmark example [42]. $c_{\rm f}$ and $c_{\rm r}$ denote the stiffness coefficients that will be introduced in (16) and (17).

1) Linear Proportional Model: In some literatures, lateral force is taken as linear proportional to the slip angle, in which the proportionality constant is called the cornering stiffness. Usually, it is written as

$$\begin{cases} F_{y\rm f} = C'_{\rm f}\alpha_{\rm f} \\ F_{y\rm r} = C'_{\rm r}\alpha_{\rm r} \end{cases} \tag{9}$$

where $F_{y\rm f}$ and $F_{y\rm r}$ are the front and rear tire forces that are perpendicular to vehicle moving direction, C'_f and C'_r are the

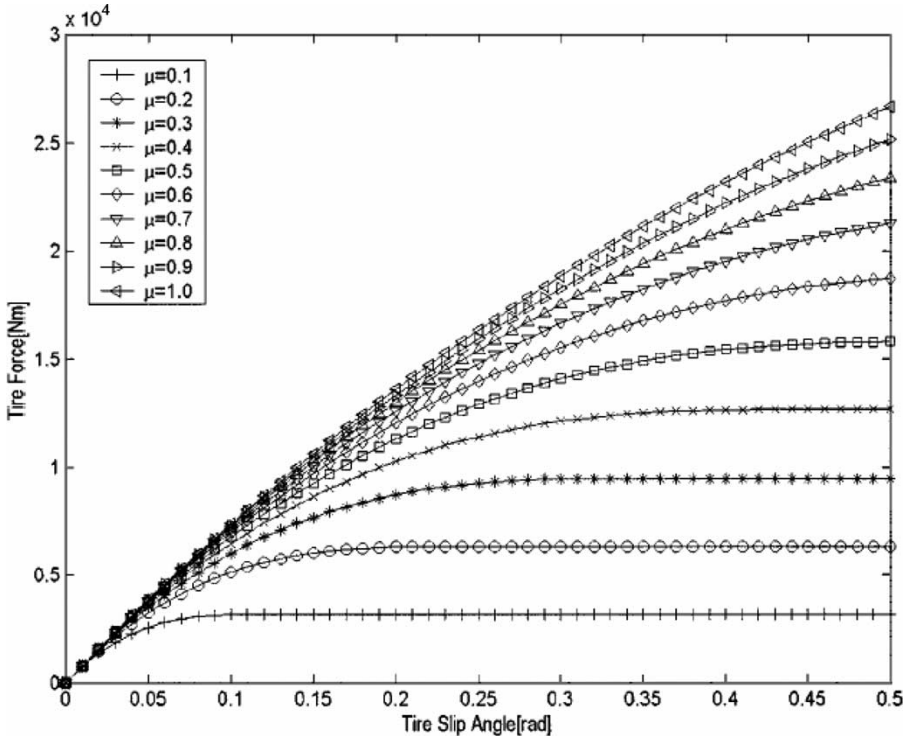

Fig. 4. Lateral tire force versus lateral slip angle [57].

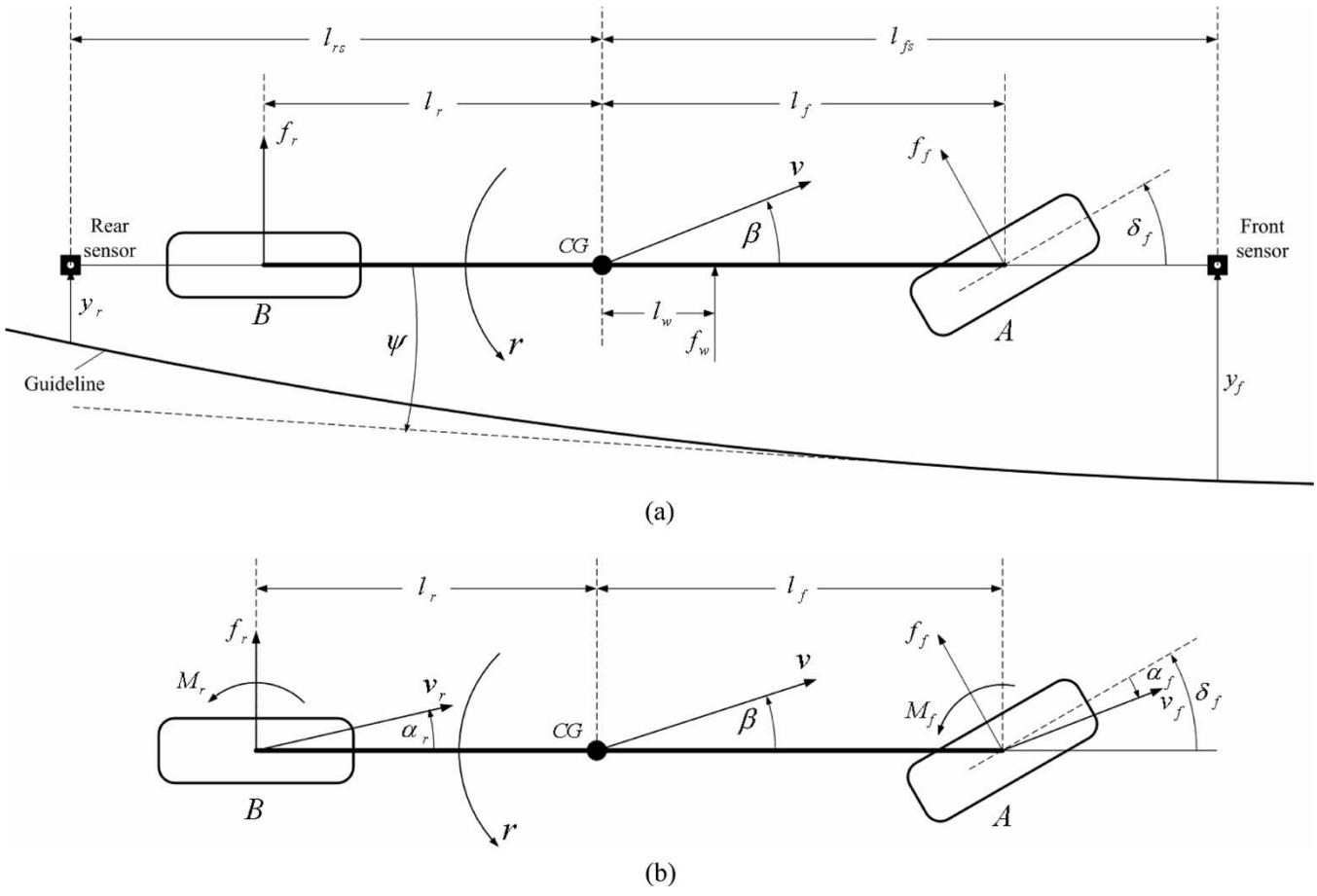

Fig. 5. "Bicycle model" for front-steering vehicles. (a) External dynamic model; (b) internal friction model.

TABLE III
PARAMETERS AND THEIR TYPICAL VALUES

Symbols	Typical values
Mass of the vehicle m	[9950, 16000]kg
Inertia moment around z-axis I_z	[10.85, 21.7]Ns/rad
Distance from A and CG l_f	3.67m
Distance from B and CG l_r	1.93m
l_{fs}	6.12m
Stiffness coefficients of front tire c_f	198000N/rad
Stiffness coefficients of rear tire c_r	470000N/rad
Acceleration of gravity force g	9.8m/(s*s)

cornering stiffness coefficients, and $\alpha_{\rm f}$ and $\alpha_{\rm r}$ are the slip angles between the orientation of the tire and the orientation of the velocity vector [see Fig. 5(b)].

Although it is not so accurate, this model gets used in some online estimation cases due to its simplicity. An example will be shown in Section V-B.

2) Nonlinear Proportional Model: To capture the saturation property of lateral tire/road friction, several nonlinear models were proposed [43], [44]. For instance, the nonlinear proportional model in [43] was chosen as

$$F_{yf} = \left[C_f'' \frac{C_{\rm f}''^2}{\mu} \frac{C_{\rm f}''^3}{\mu^2}\right] \cdot \left[|\tan\alpha_{\rm f}| \frac{-|\tan\alpha_{\rm f}|^2}{3F_z} \frac{-|\tan\alpha_{\rm f}|^3}{27F_z^2}\right]^{\rm T}. \tag{10}$$

It has been proven in several reports, e.g., [57], that such nonlinear proportional models can provide more accurate descriptions for the lateral tire/road friction phenomena and are still easy to identify.

3) Magic Formula: In [13]–[15], Bakker *et al.*, and Pacejka and Sharp developed another famous "magic formula" for the lateral tire/road friction model. Different from the above proportional models, it assumes that front tire force $f_{\rm f}$ does not only depend on front slip angle $\alpha_{\rm f}$ but also on vehicle slide slip angle β, steering angle $\delta_{\rm f}$, and read slip angle $\alpha_{\rm r}$; and so does rear tire force $f_{\rm r}$.

Normally, it is written as

$$f_{\rm f} = D_{\rm f}\sin\left\{C_{\rm f}\tan^{-1}\left(B_{\rm f}[1-E_{\rm f}]\alpha_{\rm f} + E_{\rm f}\tan^{-1}(B_{\rm f}\alpha_{\rm f})\right)\right\} \tag{11}$$

$$f_{\rm r} = D_{\rm r}\sin\left\{C_{\rm r}\tan^{-1}\left(B_{\rm r}[1-E_{\rm r}]\alpha_{\rm r} + E_{\rm r}\tan^{-1}(B_{\rm r}\alpha_{\rm r})\right)\right\} \tag{12}$$

$$\begin{cases} \alpha_{\rm f} = \beta + \tan^{-1}\left(\frac{l_{\rm f}}{v}\cdot r\cos\beta\right) - \delta_{\rm f} \\ \alpha_{\rm r} = \beta - \tan^{-1}\left(\frac{l_{\rm f}}{v}\cdot r\cos\beta\right) \end{cases} \tag{13}$$

where the coefficients B_j, C_j, D_j, and $E_j (j = f, r)$ in the models can be calculated in practice.

The "magic formula" outperforms the above two kinds of models in modeling accuracy, since it reflects the effect of yaw rate r on tire-force distribution. Moreover, it can be incorporated into the steering model to directly describe the road-surface condition.

Since lateral slide skipping forces $f_{\rm f}$ and $f_{\rm r}$ are relatively difficult to instantly measure, some recent approaches further establish some lateral tire/road friction models that do not explicitly describe lateral friction force (Table IV).

B. Bicycle Model

In 1956, Segel presented a vehicle model with three degrees of freedom to describe lateral movements including roll and yaw [39]. If roll movement is neglected, a simple model known as the "bicycle model" can be obtained. Now, this model is the most frequently used model for vehicle lateral-motion studies.

Assuming that vehicle has a constant velocity, the front-steering model can be described by the differential equations

$$\frac{d}{dt}\begin{pmatrix}\beta\\ r\end{pmatrix} = \begin{pmatrix}\frac{f_{\rm f}+f_{\rm r}}{mv} - r \\ \frac{l_{\rm f}f_{\rm f} - l_{\rm r}f_{\rm r}}{I_z}\cos\beta\end{pmatrix}. \tag{14}$$

In [45], Ono *et al.* analyzed the bifurcation phenomena in (11)–(14). Approximating the nonlinearities with

$$\cos\beta \cong 1, \quad \alpha_{\rm f} \cong \beta + \frac{l_{\rm f}}{v}\cdot r + \delta_{\rm f}, \quad \alpha_{\rm r} \cong \beta - \frac{l_{\rm f}}{v}\cdot r \tag{15}$$

they obtained the Jacobian matrix for $d/dt\binom{\beta}{r} = F(\beta, r, \delta_{\rm f})$ at equilibrium point χ_0 as

$$A_{\chi_0} = \begin{bmatrix} -\frac{c_{\rm f}^* + c_{\rm r}^*}{mv} & -1 - \frac{l_{\rm f}c_{\rm f}^* - l_{\rm r}c_{\rm r}^*}{mv^2} \\ -\frac{l_{\rm f}c_{\rm f}^* - l_{\rm r}c_{\rm r}^*}{I_z} & -\frac{l_{\rm f}^2c_{\rm f}^* + l_{\rm r}^2c_{\rm r}^*}{I_z v} \end{bmatrix} \tag{16}$$

where $c_{\rm f}^*$ and $c_{\rm r}^*$ are the tangents to slopes of front- and rear-side force characteristics at equilibrium point χ_0, respectively. The bifurcation situation around point χ_0 has been checked.

If cornering stiffness $c_{\rm f}^*$ and $c_{\rm r}^*$ are taken to be constant, the linear model for the front-steering vehicle can be written as

$$\begin{bmatrix}\dot\beta\\ \dot r\\ \dot\psi\\ \dot y_{\rm f}\\ \dot y_{\rm r}\end{bmatrix} = \begin{bmatrix} a_{11} & a_{12} & 0 & 0 & 0 \\ a_{21} & a_{22} & 0 & 0 & 0 \\ 0 & 1 & 0 & 0 & 0 \\ v & l_{\rm fs} & v & 0 & 0 \\ -v & -l_{\rm rs} & v & 0 & 0 \end{bmatrix}\begin{bmatrix}\beta\\ r\\ \psi\\ y_{\rm f}\\ y_{\rm r}\end{bmatrix} + \begin{bmatrix} b_{11} & 0 & d_1 \\ b_{21} & 0 & d_2 \\ 0 & -v & 0 \\ 0 & 0 & 0 \\ 0 & 0 & 0 \end{bmatrix}\begin{bmatrix}\delta_{\rm f}\\ \rho_{\rm ref}\\ f_{\rm w}\end{bmatrix} \tag{17}$$

where

$$a_{11} = -\frac{(c_{\rm r}+c_{\rm f})}{\widetilde{m}v},\ a_{12} = -1 + \frac{(c_{\rm r}l_{\rm r} - c_{\rm f}l_{\rm f})}{\widetilde{m}v^2}$$
$$a_{21} = \frac{(c_{\rm r}l_{\rm r} - c_{\rm f}l_{\rm f})}{\widetilde{I}_z},\ a_{22} = -\frac{\left(c_{\rm r}l_{\rm r}^2 + c_{\rm f}l_{\rm f}^2\right)}{\widetilde{I}_z v}$$
$$b_{11} = \frac{c_{\rm f}}{\widetilde{m}v},\ b_{21} = \frac{c_{\rm f}l_{\rm f}}{\widetilde{I}_z},\ d_1 = \frac{1}{mv},\ d_2 = \frac{l_{\rm w}}{I_z}.$$

Here, $\widetilde{m} = m/\lambda$ and $\widetilde{I}_z = I_z/\lambda$ are the normalized mass and inertia, respectively, and λ is a controllable parameter to

TABLE IV
SOME REPRESENTATIVE LATERAL TIRE/ROAD FRICTION MODELS

Year	Model Name	Model Properties	Features
	Linear Proportional Model	Empirical	1. Cannot accurately reflect saturation properties 2. Easy to identify
	Nonlinear Proportional Model	Semi-Empirical	1. Can accurately fit curves 2. Has several different formula
1987	Magic Formula	Semi-Empirical	Can accurately fit curves
	Bicycle Model	Analytical	Does not reflect tire/road friction force directly

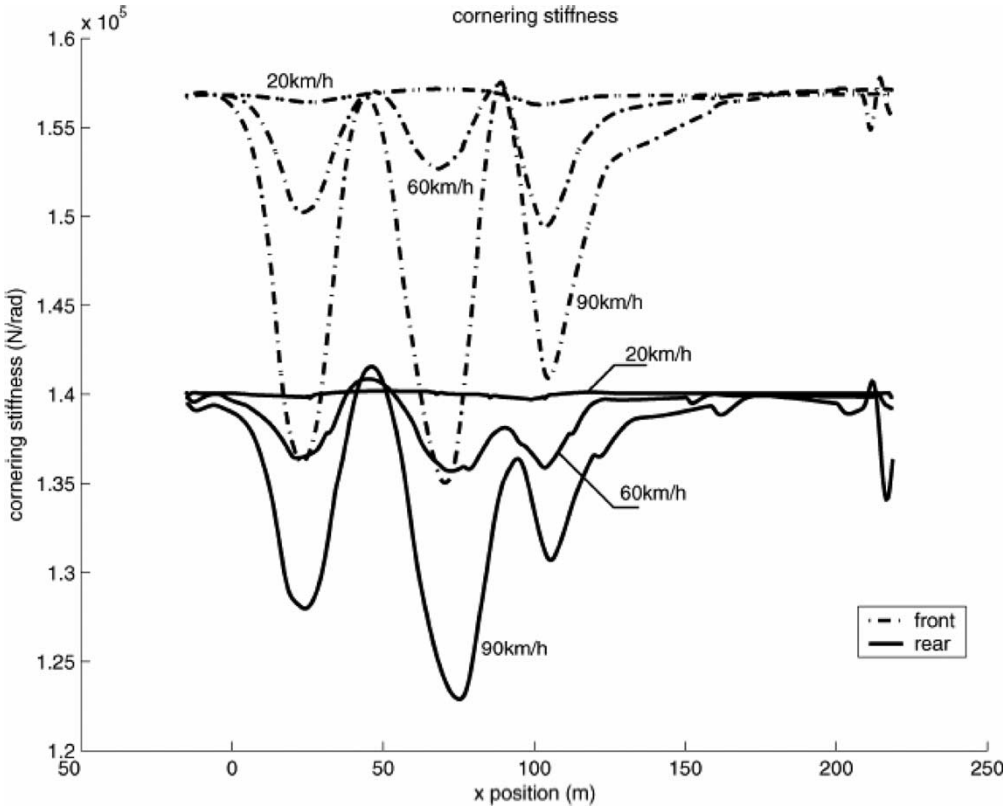

Fig. 6. Variation of rear and front cornering stiffness at speeds of 20, 60, and 90 km/h [46].

model road-adhesion factor with $\lambda = 1$ for a dry road and $\lambda = 0.5$ for a wet road.

The "bicycle model" can also be viewed as a certain lateral tire/road friction model, in which the friction situation is described by two stiffness coefficients $c_{\rm f}$ and $c_{\rm r}$. Based on vehicle movement information, $c_{\rm f}$ and $c_{\rm r}$ can be estimated and monitored online. Some related reports will be discussed in Section V-D.

Cornering stiffness varies with several factors. One factor is that it increases with tire pressure. When the car turns, the mass transfer onto the external wheels increases tire pressure, which can lead to notable variations in cornering stiffness. As shown in Fig. 6, Stephant *et al.* showed in [46] that the variations caused by this factor are normally less than 10% and still tolerable for most robust steering controllers [11].

In addition, a front-steering vehicle's unstabilization was revealed in [45] to be caused by a saddle-node bifurcation, which depends heavily on the rear-tire-side force saturation. Thus, full-steering vehicles naturally outperform front-steering vehicles in handling and stability [47]–[49].

Besides the above models, there were some other lateral tire models proposed, e.g., [50]. However, researchers gradually realized that integrated models that consider both longitudinal and lateral tire/road friction can describe the friction phenomena more accurately. As a result, more and more efforts are put into integrated tire/road friction modeling recently.

IV. INTEGRATED TIRE/ROAD FRICTION MODELING

A. Integrated Tire/Road Friction Characteristics

Let us use F_y to denote lateral friction force. Then, the lateral tire/road friction coefficient could be defined as

$$\mu_y = \frac{F_y}{F_z}. \tag{18}$$

Fig. 7 shows the dependence relationships of $\mu_x - s_x$ and $\mu_y - s_y$, respectively. It is clear that lateral force F_y notably depends on side slip angle α. The larger the side slip angle is, the smaller the lateral force gets. This property can be used in ABS design. An example of it is discussed in Section VI.

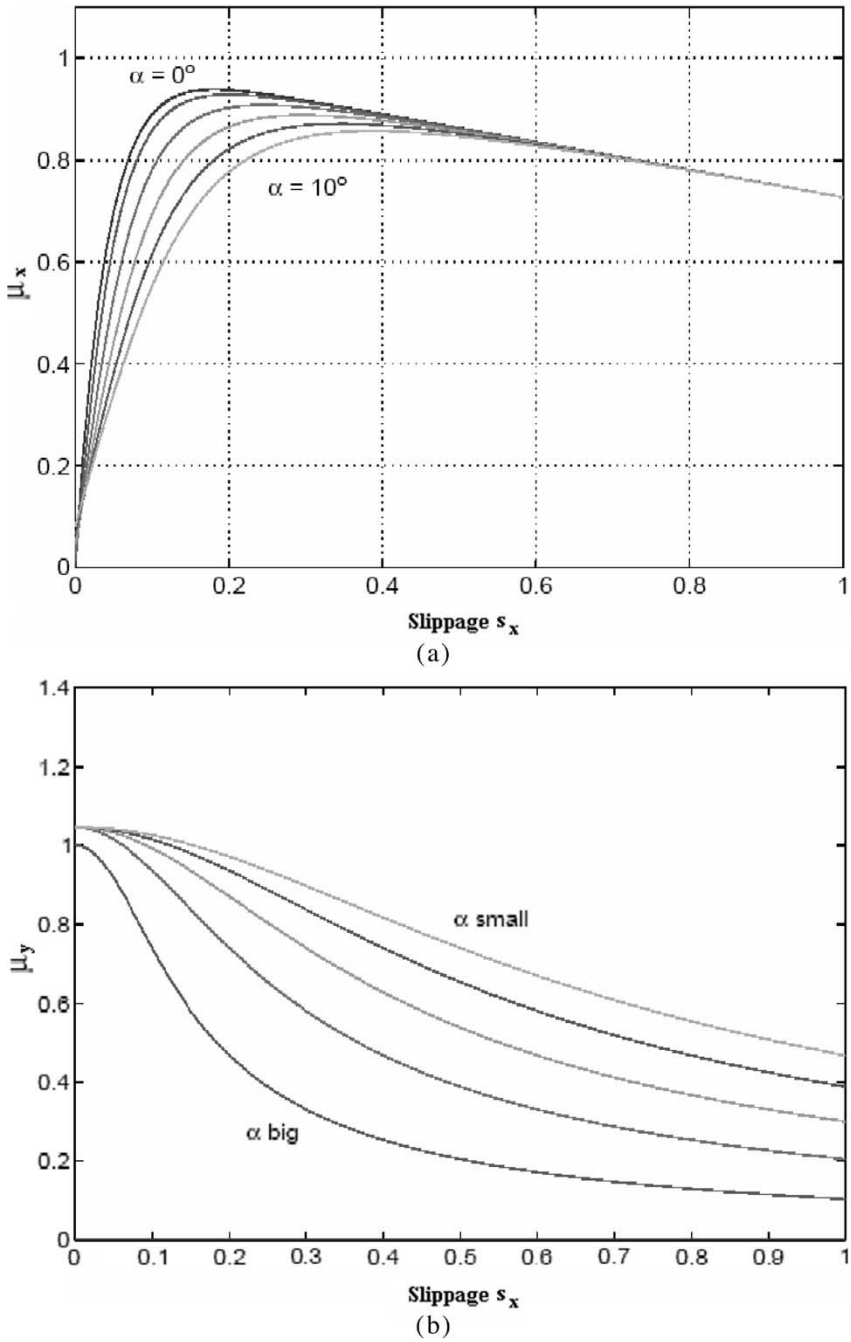

Fig. 7. Typical tire side slip/friction curves. (a) $\mu_x - s_x$; (b) $\mu_y - s_x$[51].

B. Empirical and Semiempirical Integrated Models

There have been several different empirical and semiempirical integrated models proposed in the last 10 years [52]–[58]. Usually, these models first decompose the whole friction force into two orthogonal parts, longitudinal and lateral force (see Fig. 8). Then, longitudinal and lateral forces are represented as a function in terms of μ_x/μ_y (or s_x/s_y) and side slip angle α.

For instance, in the Kiencke model that was proposed in [9], the longitudinal force is written as

$$F_x = \mu \frac{F_z}{g} \left[g_x \cos(\alpha) - k_{\mu y} g_y \sin(\alpha) \right] \tag{19}$$

and the lateral force is written as

$$F_y = \mu \frac{F_z}{g} \left[g_x \sin(\alpha) + k_{\mu y} g_y \cos(\alpha) \right] \tag{20}$$

where α denotes the slip angle α_{f} or α_{r}, F_z is the vertical pressure force generated by vehicle load, μ is the common friction coefficient that is associated with s_x, and g_l/g and $k_{\mu \mathrm{t}} g_{\mathrm{t}}/g$ represent the longitudinal and lateral (transversal) decomposition coefficients, respectively.

To approximate the nonlinear properties of tire/road friction, recent empirical models have become increasingly complex, e.g., the models proposed in [57].

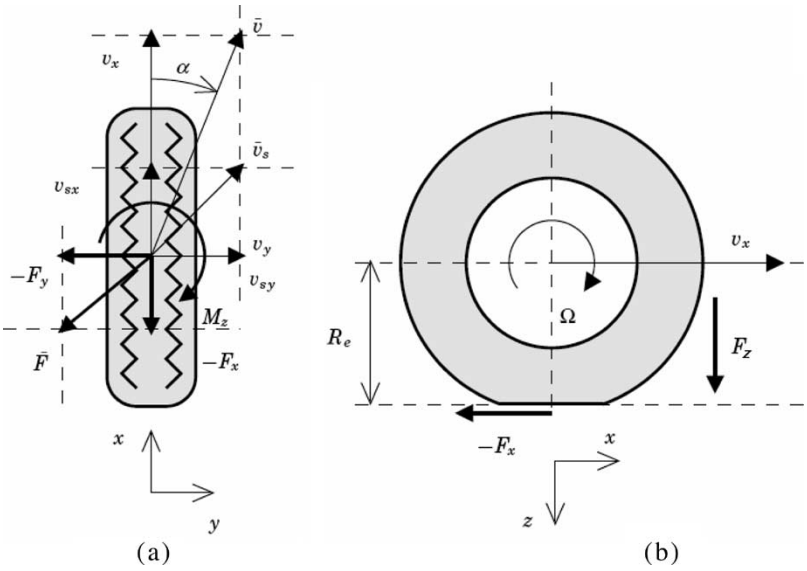

Fig. 8. Kinematics of a tire during braking and cornering. (a) Top view; (b) side view, partly from [66].

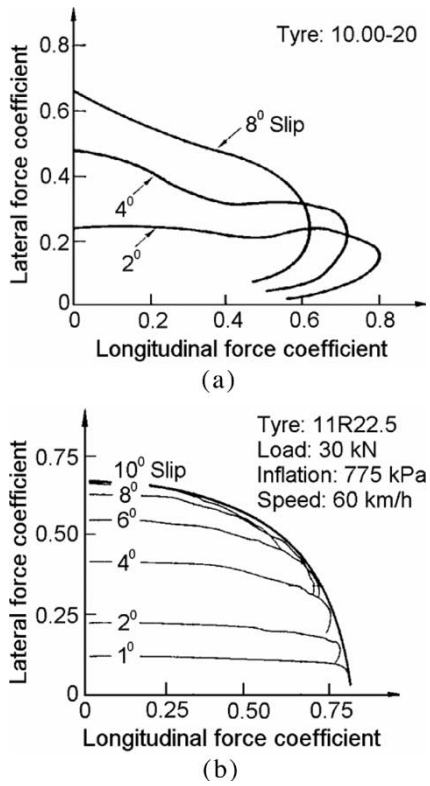

Fig. 9. Braking and cornering. (a) Bias tire [64] and (b) radial tire [65].

In some recently developed models, the forces generated by deformation and adhesion are considered separately [66]. This provides the possibility to analyze the nonorthogonal distribution phenomena of tire force (see Fig. 9). The orthogonal distribution of tire force indicates a quart eclipse curve as the envelope curve shown in Fig. 9(b); however, the real curve does not fit a quart eclipse, especially for those bias tires.

For example, a new tire-force model for both braking and cornering was presented in [66], which is based on combining empirical models for pure braking and cornering with brush-model tire mechanics. The contact patch between the tire and the road is divided into an adhesion region, where the rubber is gripping the road, and a sliding region, where the rubber slides on the road surface. The total force generated by the tire is then composed of components from these two regions.

C. Analytical Integrated Models

Compared to empirical integrated models, analytical ones received much less consideration [59]–[63], among which the brush models are the most important approaches.

In order to explain tire/road friction phenomena when the vehicle simultaneously makes lateral steering and longitudinal motion, Claeys *et al.* extended the above two-dimensional (2-D) LuGre-type model into a three-dimensional (3-D) model in [60] and [61].

In the new model, wheel velocity is featured and projected into two orthogonal components, which are denoted as v_x and v_y. The microscopic bristle deflections are represented by two components z_x and z_y, respectively.

For the rigid tire belt, the extended distributed model is given by

$$\begin{cases} \frac{d\delta z_x}{dt}(\varsigma,t) = v_{x\mathrm{r}} - \sigma_0 \frac{|v_{x\mathrm{r}}|}{g(v_{x\mathrm{r}})}\delta z_x \\ \frac{d\delta z_y}{dt}(\varsigma,t) = v_{y\mathrm{r}} - \sigma_0 \frac{|v_{y\mathrm{r}}|}{g(v_{y\mathrm{r}})}\delta z_y \\ F_x = \int\limits_0^L \delta F_x d\varsigma = \int\limits_0^L \left(\sigma_{x0}\delta z_x + \sigma_{x1}\frac{d\delta z_x}{dt} + \sigma_{x2}v_x\right)\delta F_n d\varsigma \\ F_y = \int\limits_0^L \delta F_y d\varsigma = \int\limits_0^L \left(\sigma_{y0}\delta z_y + \sigma_{y1}\frac{d\delta z_y}{dt} + \sigma_{y2}v_y\right)\delta F_n d\varsigma \end{cases} \tag{21}$$

where

$$g(v_{x\mathrm{r}}) = \mu_{x\mathrm{c}} + (\mu_{x\mathrm{s}} - \mu_{x\mathrm{c}})\mathrm{e}^{-\left|\frac{v_{x\mathrm{r}}}{v_{x\mathrm{s}}}\right|^{\frac{1}{2}}}$$

$$g(v_{y\mathrm{r}}) = \mu_{x\mathrm{c}} + (\mu_{x\mathrm{s}} - \mu_{x\mathrm{c}})\mathrm{e}^{-\left|\frac{v_{y\mathrm{r}}}{v_{y\mathrm{s}}}\right|^{\frac{1}{2}}}.$$

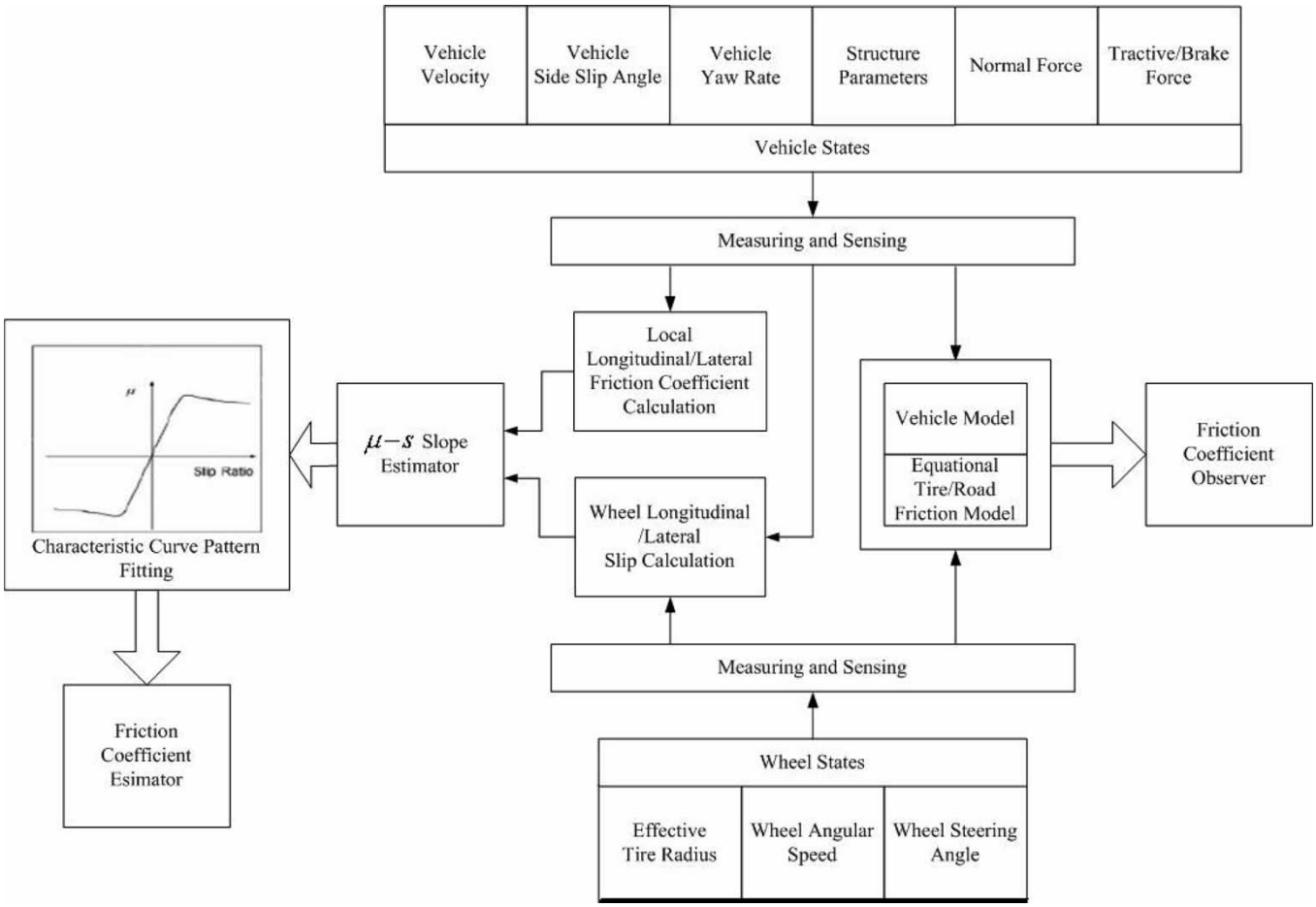

Fig. 10. Scheme of the tire/road friction monitor.

All the symbols above have similar meanings to those given for the 2-D LuGre model except foot notes x and y denote longitudinal and lateral directions, respectively.

One apparent shortcoming of this 3-D LuGre model is its distributed formulation. Several convenient conclusions given for the 2-D LuGre Model cannot be directly employed into this 3-D model. Several studies were carried out to get the approximate lumped friction model, e.g., [62], [63], and [67]. However, all these approaches still need further discussions.

V. Tire/Road Friction Monitors

A. Scheme and Sensors for Tire/Road Friction Monitors

A general scheme of the tire/road friction monitor is shown in Fig. 10. It is obvious that correct information of vehicle position, velocity, wheel speed, and steering angle need to be measured before an acceptable estimation of the frictions is obtained.

Since a vehicle is a highly complex system that is composed of varied mechanical, electronic, and electromechanical elements, numerous sensors were designed and applied to measure the movement information.

There are three position systems: inertial navigation system (INS), global positioning system (GPS), and magnetic positioning system (MPS), that are used in IV projects. INS is the first position-navigation system used worldwide, and the corresponding techniques had been invented and applied since World War II [68]. With the fast development of manufacturing techniques, classic mechanical inertial position sensors have become more and more accurate. Some useful measurement-error handling techniques are proposed as well. However, mechanical inertial gyroscopes consume relatively high power and are vulnerable to damage.

Recently, a so-called "solid-state" solution was proposed with the developing of optical theory and microchip industry [69]. Such new-type INSs are realized by using discrete integrated electronic-mechanical or electronic-optical sensors only. Since they have no moving parts, such new-type INSs outperform the conventional INS in many ways. Some attempts towards on-vehicle optical INS have already been reported in [70].

Applications of GPS for vehicle-position measurements are reported worldwide. The current trend is to combine INS and GPS together to achieve better performance [71], [72].

Magnetic sensing is another promising technology that has been developed recently for the purposes of vehicle-position measurement and guidance. By using either magnetic tapes or magnetic markers, the vehicle position can be obtained as well as some other useful information, e.g., vehicle slip angle [73]–[75].

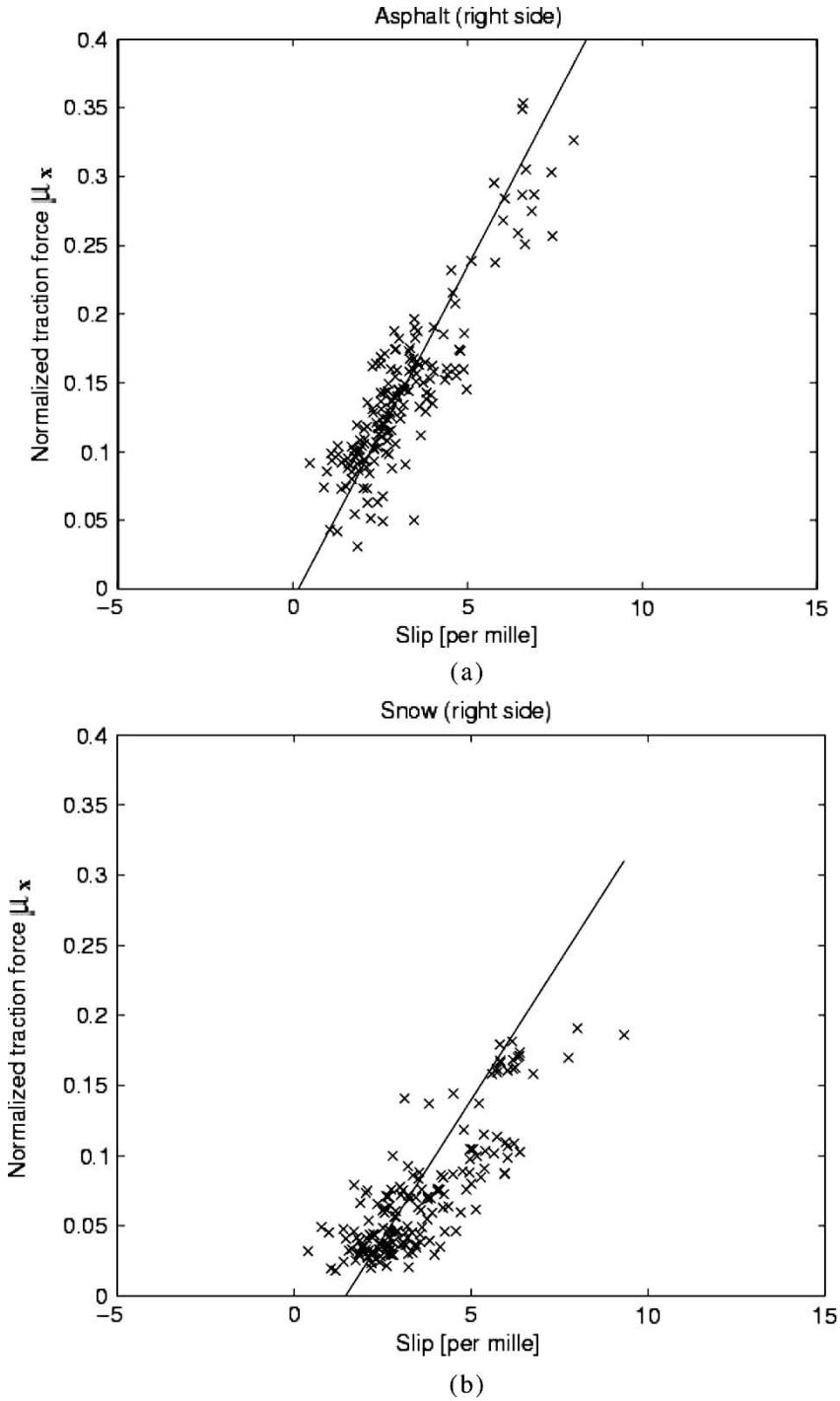

Fig. 11. Samples of u and s computed from ABS signals on the right side of the car (a) on dry asphalt and (b) hard snow, respectively. Crosses denote measurements and the solid line is a straight-line approximation [81].

In addition, vision sensors can also be employed to measure motion. For example, the offset between the vehicle and curve can be accurately obtained by using the laser sensor proposed in [76]. However, its measurement performance is more vulnerable to environmental disturbances, e.g., fog.

However, not all vehicle characteristics are directly measured due to high cost or some other reasons. Instead, several special observers are used to reconstruct the needed information. In literatures, these observers were also called virtual sensors [46].

B. Identification of Empirical Longitudinal Friction Models

Online identification for empirical longitudinal tire/road friction models have been studied since the early 1990s [77]–[80].

In [81] and [82], Gustafsson proposed a linear regression model for the tire/road friction status monitor, which emphasized the slip slope of the friction only. As shown in Fig. 11, he considered the slippage s_x to be a linear function of μ_x as

$$s_x = \frac{1}{k}\mu_x + \delta \tag{22}$$

where $1/k$ is used to represent the slip slope and δ is used to compensate the offset.

Apparently, this much-simplified model neglects all the dynamic features of tire/road friction. However, it is very easy to put into use. Gustafsson tested this filter on a Volvo 850, and proved that the alarm time after a change is in the order of a second. However, as shown in Fig. 11, the estimation error is still considerable.

There have been some other more complex identification models. In [84], the empirical identification model is chosen as

$$\mu_x = \mu_0' \frac{s_x}{c_1 s_x^2 + c_2 s_x + 1} \tag{23}$$

where μ_0', c_1, and c_2 are parameters that need to be identified.

In [83], Muller *et al.* proposed the following semiempirical model for identification

$$\mu_x = 3\gamma s_x - \frac{3\gamma^2}{\mu_0} s_x^2 \frac{s_x}{|s_x|} + \frac{\gamma^3}{\mu_0^2} s_x^3 \tag{24}$$

where $\gamma = 4a^2 bk/3F_z$ is a predefined coefficient, and a and b are the length and width of the rectangle contact area. They all need to be estimated, including μ_0.

Besides the above ones, there are many other empirical/semiempirical nonlinear estimation models proposed to approach the tire/road curve more accurately [85], [86]. However, none of them can directly employ and describe dynamic properties of tire/road friction.

C. Observer of Analytical Longitudinal Friction Models

Different from empirical models, analytical longitudinal tire/road friction models, which are usually described by differential equations, require the observers to monitor friction changes [87]–[93].

For example, Canudas de Wit and Horowitz developed an observer for the 2-D LuGre model in [89], in which the uncertainty was modeled by introducing a new parameter θ as

$$\begin{cases} \frac{dz}{dt} = v_{\mathrm{r}} - \theta\sigma_0 \frac{|v_{\mathrm{r}}|}{g(v_{\mathrm{r}})} z \\ v_{\mathrm{r}} = v_x - r\omega \\ F_x = \left(\sigma_0 z + \sigma_1 \frac{dz}{dt} + \sigma_2 v_{\mathrm{r}}\right) F_{xn} \end{cases} \tag{25}$$

where different road-adhesion coefficients can be represented by different θ's. Thus, the problem of monitoring tire/road friction can be reformulated as the online estimation problem of θ.

The vehicle dynamics can be written as

$$\begin{cases} F_x = \frac{m\dot{v}_x}{4} \\ J\dot{\omega} = -rF_x + u \end{cases} \tag{26}$$

where r is the inertia and radius of the wheel and u denotes the accelerating or braking torque.

Combining (24) and (25), Canudas de Wit *et al.* introduced the following transformation as

$$\begin{cases} \eta = rmv + J\omega \\ \chi = J\omega + rF_n\sigma_1 z \end{cases} \tag{27}$$

and the output was chosen as $\xi = (1/J)[\varsigma_2 - rF_n\sigma_1\varsigma_3] = \omega$.

Thus, the longitudinal vehicle dynamic model is written as

$$\begin{cases} \dot{\varsigma} = \widetilde{A}\varsigma + \widetilde{B}\left[\theta\varphi(\xi, u, \varsigma)\right] + \widetilde{R}u + \widetilde{E}\xi \\ \dot{\theta} = 0 \\ \xi = \widetilde{C}\varsigma \end{cases} \tag{28}$$

where $\varsigma = [\eta \quad \chi \quad z]^{\mathrm{T}}$ are the transformed state variables, and $\widetilde{A}$, $\widetilde{B}$, $\widetilde{C}$, and $\widetilde{E}$ are the corresponding matrices.

Notice that there exists a function $q(\cdot)$ for the LuGre model, in which

$$\left|\varphi(\hat{\xi}, u, \hat{\varsigma})\right| \le q(\hat{\varsigma}) \le q_{\max}$$

the following observer was proposed in [81]

$$\begin{cases} \dot{\hat{\varsigma}} = \widetilde{A}\hat{\varsigma} + \widetilde{B}\left[\hat{\theta}\varphi(\hat{\xi}, u, \hat{\varsigma})\right] + \widetilde{E}u + \widetilde{K}(\xi - \hat{\xi}) + \widetilde{B}\eta \\ \hat{\theta} = \gamma\varphi(\hat{\varsigma})\hat{\xi} \\ \hat{\xi} = \widetilde{C}\hat{\varsigma} \end{cases} \tag{29}$$

where $\eta = 2\hat{\theta}_{\max}(q_{\max} + q(\|\hat{\varsigma}\|^2))\mathrm{sgn}(\hat{\xi})$.

It was proven in [89]–[91] that θ can be correctly estimated using (29) if the wheel angular velocity ω can be measured. A typical simulation result is shown in Fig. 12, where θ is varied from 1 to 4 to mimic different road-surface conditions. It was further shown in [92] that this method can be extended to build a fault-detection observer with respect to disturbance caused by unsteady road surface or unavoidable vehicle vertical vibration.

D. Identification of Empirical Lateral Friction Models

There are several discussions on empirical lateral tire/road friction identification [57], [94]–[102].

In [95], lateral tire friction forces were estimated using the simple cornering stiffness model as

$$\begin{cases} C_{\mathrm{f}}' = \frac{F_{y\mathrm{f}}}{\alpha_{\mathrm{f}}} \\ C_{\mathrm{r}}' = \frac{F_{y\mathrm{r}}}{\alpha_{\mathrm{r}}} \end{cases} \tag{30}$$

where the lateral forces are calculated as

$$\begin{cases} m\dot{v}_y = F_{y\mathrm{f}} + F_{y\mathrm{r}}\cos(\delta_{\mathrm{f}}) \\ I_z\ddot{\psi} = l_{\mathrm{f}}F_{y\mathrm{f}} - l_{\mathrm{r}}F_{y\mathrm{r}}\cos(\delta_{\mathrm{f}}) \end{cases} \tag{31}$$

and the side slip angles are tracked using GPS signals as

$$\begin{cases} \phi = \tan^{-1}\left(\frac{v_y}{v_x}\right) \\ \alpha_{\mathrm{f}} = \phi - \delta_{\mathrm{f}} \\ \alpha_{\mathrm{r}} = \phi \end{cases}. \tag{32}$$

In [97], Sienel proposed a recursive derivation formula of the lateral friction coefficients in terms of previous measurement

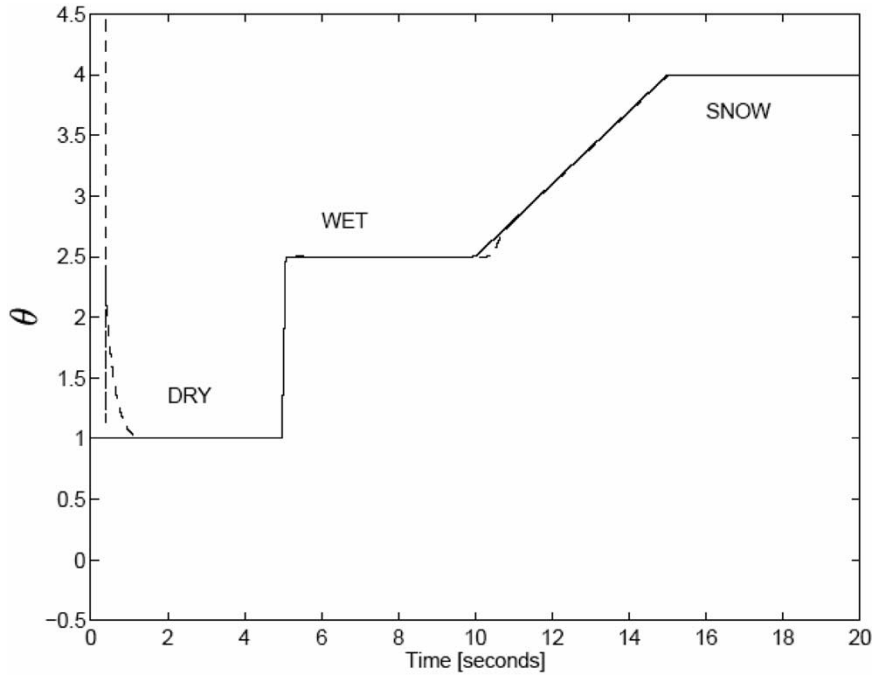

Fig. 12. Estimation result of varied θ [89].

for rotation and lateral acceleration, where $\alpha_{\rm f}$ is tracked as

$$\dot{\alpha}_{\rm f} = \dot{\delta}_{\rm f} - \frac{\alpha_{\rm f}}{v} + r. \tag{33}$$

At sampling time i, $C'_{{\rm f},i}$ is estimated as

$$C'_{{\rm f},i} = \begin{cases} m \cdot \frac{l_{\rm r}}{l_{\rm f}+l_{\rm r}} \cdot \frac{\dot{\alpha}_{{\rm f},i}}{\dot{\delta}_{\rm f} - \frac{\alpha_{\rm f}}{v} + r}, & \text{for } \left|\dot{\delta}_{{\rm f},i} - \frac{\alpha_{{\rm f},i}}{v_i} + r_i\right| > \varepsilon \\ C'_{{\rm f},i-1}, & \text{else.} \end{cases} \tag{34}$$

Apparently, it requires the measurement of yaw rate r additionally with respect to the above method.

In [98], the cornering stiffness coefficients are estimated by

$$\begin{cases} C'_{\rm f} = C'_{\rm f0}\left(1 - \frac{\dot{v}}{\mu_{\rm f} g}\right) \\ C'_{\rm r} = C'_{\rm r0}\left(1 - \frac{\dot{v}}{\mu_{\rm r} g}\right) \end{cases} \tag{35}$$

where $\mu_{\rm f}$ and $\mu_{\rm r}$ are the common adhesion coefficients, and $C'_{\rm f0}$ and $C'_{\rm r0}$ are the bound values.

There were also some integrated estimation models that had been proposed. In [99] and [100], Ray used extended Kalman–Bucy filtering and Bayesian hypothesis selection to estimate motion, tire forces, and tire/road friction coefficient on asphalt surface. It requires no *a priori* knowledge of friction coefficients and does not require a tire-force model. It first estimates tire friction based on measurement of vehicle motion and then determines friction. Similar methods are also reported in [101] and [102].

VI. Tire/Road Friction Models and ABS Design

ABS for commercial vehicles first appeared on the market in the 1960s and began its fast growth in the 1970s with the emergence of computers and electronics technologies [103]–[106]. Now, ABS has been recognized as an important contribution to road safety. It is available in almost all types of modern vehicles.

The advantage of ABS can be clearly seen when comparing the emergency braking situation of vehicles with and without ABS. When the driver wants to reduce the speed of the vehicle, the wheels of the vehicle without ABS will lock and the vehicle will start sliding, which leads to some undesirable effects. One reason is that the tire wear will not be equally distributed over the whole tire. Another is that the vehicle becomes unsteerable as soon as the wheels lock. This might be quite dangerous in the case when the driver wants to avoid an obstacle during the braking maneuver. In a vehicle with ABS, sensors can monitor the rotation of the wheels and reduced the brake pressure if the wheels are locked. Thus, the wheels are still rolling and steerable, and a high tire/road friction is simultaneously achieved.

A general scheme of ABS is shown in Fig. 13. In the past 40 years, a great number of ABSs based on varied tire/road friction models have been proposed.

A. ABS Based on Longitudinal Tire/Road Friction Models

There have been several approaches based on piecewise linear tire/road friction models [107], [108]. For instance, in [107], Schinkel and Hunt designed an ABS by approximating $\mu_x(s_x)$ with piecewise linear functions

$$\begin{cases} \mu_x = a s_x, & s_x \le 0.1 \\ \mu_x = -\frac{1}{4} s_x + \frac{3}{4} \pm 0.2, & s_x > 0.1 \end{cases} \tag{36}$$

where a was chosen as $a \in [5.75, 9.75]$. The notation ± 0.2 means that any arbitrary unfixed value should lie in the boundary interval $(-0.2, 0.2)$.

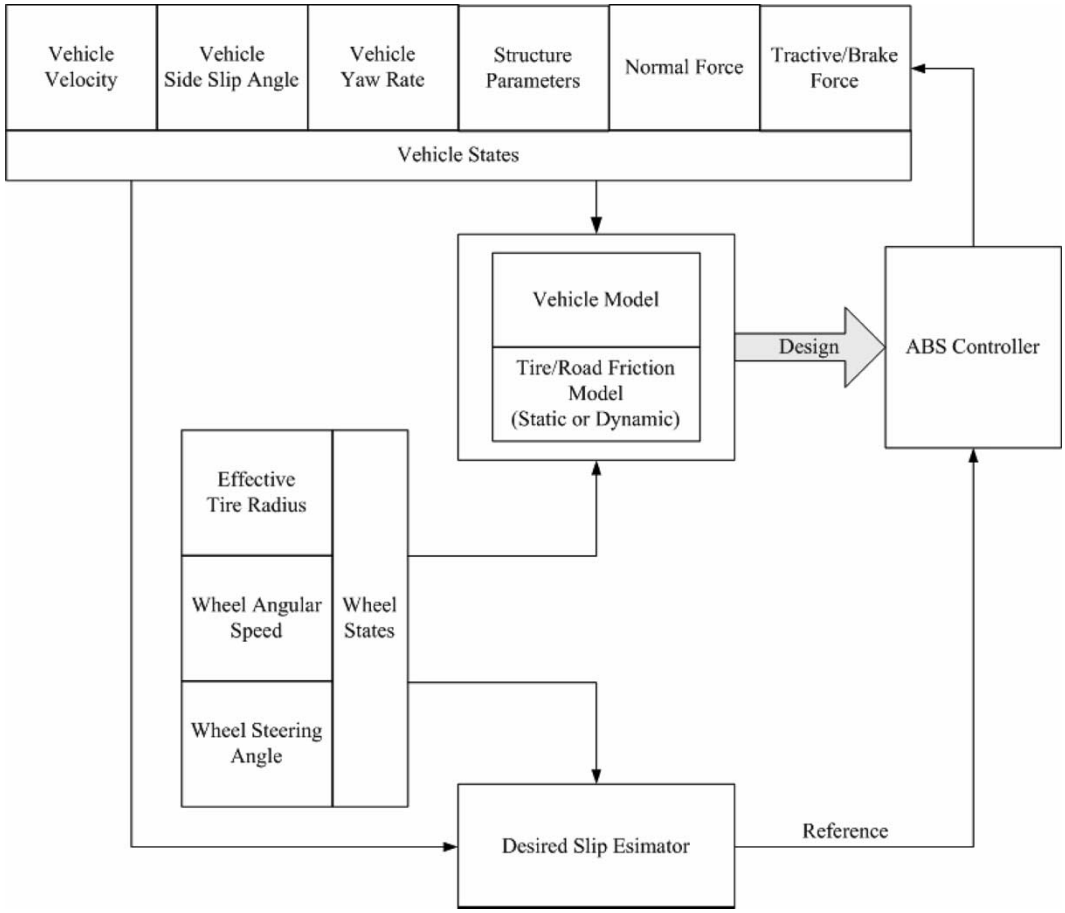

Fig. 13. Scheme of ABS.

They formulated the quarter car braking model as

$$\begin{cases} \dot{s}_x = -\frac{1}{v_x}\left[\frac{1}{m}(1-s_x)+\frac{r^2}{J}\right]F_z\mu(s_x)+\frac{1}{v_x}\frac{r}{J}T_{\rm b} \\ \dot{v} = -\frac{1}{m}F_z\mu(s_x) \end{cases}. \quad (37)$$

They proved that a sliding-mode controller

$$\dot{s} = -\frac{r^2F_z\mu_x(s_x)}{v_xJ}+\frac{1}{v_x}\frac{r}{J}T_{\rm b}+Ke \quad (38)$$

can guarantee the stability of the error system $e=\lambda-\lambda_{\rm d}$, with the sliding surface chosen as $s=((d/dt)+K)\int_0^t e d\tau$.

Here, $T_{\rm b}$ is determined as

$$\begin{cases} \hat{T}_{\rm b} = 10rF_z\lambda+\frac{vJ}{r}Ke, & s_x \le 0.08 \\ \hat{T}_{\rm b} = -\frac{sK_{\rm p}+K_i}{s}e, & 0.08 \le s_x \le 0.12 \\ \hat{T}_{\rm b} = \left(-\frac{1}{4}\lambda+\frac{3}{4}-0.2\right)rF_z-\frac{vJ}{r}Ke, & s_x > 0.12. \end{cases} \quad (39)$$

Some recent approaches applied more accurate empirical models in ABS design [19]. For example, the "magic formula" was used in [109] and [110]. The major drawback of such static analysis is based on the assumption that the friction force between the tire and the ground can be accurately described as a static relation in terms of the slip coefficient. However, it is well known that transient phenomena are quite important for ABS.

In [90] and [91], a control scheme utilizing the LuGre dynamic friction model to estimate the tire/road friction for emergency braking of vehicles is designed. The control-system output is the pressure to the braking system, and is calculated using only the wheel angular speed. The controller utilizes estimated state feedback control to achieve near-maximum deceleration. The state observer gain is calculated by using linear matrix inequality (LMI) techniques. It is proven that it outperforms similar optimal control based on the static model given in [109].

Moreover, as pointed out in [109], the static-friction approach also requires *a priori* knowledge of the maximum friction force and the corresponding optimal slip, which may not be readily known in a realistic environment of changing road and tire conditions. This drawback can be avoided by implementing the optimal strategy via an "extremum-seeking" control scheme, such as the methods proposed in [111] and [112].

B. ABS Based on Integrated Tire/Road Friction Models

The phenomenon shown Fig. 7(b) inspires a motivation for ABS brakes, since avoiding high longitudinal slip values will maintain high steerability and lateral stability of the vehicle

during braking. Achieving this by manual control is difficult, because the slip dynamics are fast and open-loop unstable when operating at wheel slip values to the right of any peak of the friction curve. We expect that a reasonable tradeoff between high longitudinal friction F_x and lateral friction F_y is achieved under all road conditions for longitudinal slip s_x close to its peak value on the longitudinal slip curve.

There have been some attempts in this direction using empirical models, e.g., [51], [113], and [114]. For example, in [51], the above ABS control model (37) was modified as

$$\begin{cases} \dot{s}_x = -\frac{1}{v_x}\left[\frac{1}{m}(1-s_x)+\frac{r^2}{J}\right]F_z\mu(s_x,\alpha)+\frac{1}{v_x}\frac{r}{J}T_{\mathrm{b}} \\ \dot{v} = -\frac{1}{m}F_z\mu(s_x,\alpha) \end{cases} \tag{40}$$

which address the effects of side slip angle α.

However, the system dynamics become quite complex after considering α, and further efforts need to be carried out.

VII. Concluding Remarks

The recent trend of research on developments of tire/road friction modeling and related control techniques is reviewed in this paper. It sequentially studies the previous research efforts in longitudinal/lateral/integrated tire/road friction modeling and discusses their applications in recent vehicle traction, steering, and braking controller/observer designs.

However, some important contents were left untouched in this paper due to space limitations. For instance:

1) The tire/road friction-estimation methods based on torque converter/powertrain models [115], [116] are not discussed here. For instance, the force axis of the slip curve was estimated from an observer based on the model of the torque converter in [115].
2) Some novel tire/road modeling methods, which uses neural networks or some other techniques to "learn" the nonlinear characteristics of friction phenomena, are not mentioned in this paper [117]. Additionally, the algorithms for tire/road friction-model parameter identification [118], [119], such as the identification algorithm using genetic algorithms (GAs) that were proposed in [119], are not discussed here either.
3) In this paper, it is assumed that the vehicles are moving on a flat surface and their vertical-position changes are neglected. However, this simplification may yield notable errors in some cases. The methods that were developed to deal with such situations, e.g., [120], are not examined.
4) In this paper, the tire/road friction force is indirectly measured via the resulting vehicle motion. It uses the tire as a "virtual" sensor, as what was summarized in [121]. Recently, some novel tire sensors, e.g., surface acoustic wave (SAW) sensors [122], [123], were proposed to directly measure tire deformation and temperature [124], and therefore determine tire/road friction force. How to employ these "real" sensors in tire/road friction modeling, monitoring, and control issues is expected to become a hot topic of this field in the near future.

References

[1] R. Larsen, "AVCS: An overview of current applications and technology," in *Proc. Intelligent Vehicles Symp.*, Detroit, MI, 1995, pp. 152–157.
[2] R. Bishop, "A survey of intelligent vehicle applications worldwide," in *Proc. IEEE Intelligent Vehicles Symp.*, Dearborn, MI, 1995, pp. 25–30.
[3] U. Kiencke, "Future perspectives of automotive control," in *Proc. 18th IEEE Instrumentation and Measurement Technology Conf.*, Budapest, Hungary, 2001, vol. 3, pp. 1510–1518.
[4] D. F. Moore, *The Friction of Pneumatic Tyres*. New York: Elsevier, 1975.
[5] T. French, *Tyre Technology*, A. Hilger, Ed. Bristol, U.K., 1989.
[6] D. Dowson, *History of Tribology*. London, U.K.: Longman, 1998.
[7] B. Feeny, A. Guran, N. Hinrichs *et al.*, "A historical review on dry friction and stick-slip phenomena," *ASME Appl. Mech. Rev.*, vol. 51, no. 5, pp. 321–341, May 1998.
[8] J. Y. Wong, *Theory of Ground Vehicles*. New York: Wiley, 1993.
[9] U. Kiencke and L. Nielsen, *Automotive Control System for Engine, Driveline, and Vehicle*. Berlin, Germany: Springer-Verlag, 2000.
[10] W. Hirschberg, G. Rill, and H. Weinfurter, "User-appropriate tyre-modelling for vehicle dynamics in standard and limit situations," *Veh. Syst. Dyn.*, vol. 38, no. 2, pp. 103–125, Feb. 2002.
[11] L. Li and F.-Y. Wang, "Research advances in vehicle lateral motion monitoring and control," *Int. J. Intell. Control Syst.*, vol. 10, no. 1, pp. 60–76, Mar. 2005.
[12] J. Harned, L. Johnston, and G. Scharpf, "Measurement of tire brake force characteristics as related to wheel slip (anti-block) control system design," *SAE Trans.*, vol. 78, no. 690214, pp. 909–925, 1969.
[13] E. Bakker, L. Nyborg, and H. B. Pacejka, *Tire Modeling for Use in Vehicle Dynamic Studies*, 1987, Warrendale, PA: Soc. Automotive Eng. SAE 870421.
[14] E. Bakker, H. B. Pacejka, and L. Lidner, "A new tire model with an application in vehicle dynamics studies," presented at the Int. Congr. and Expo., Detroit, MI, 1989, SAE Paper 890087.
[15] H. B. Pacejka and R. S. Sharp, "Shear force development by pneumatic tires in steady state conditions: A review of modeling aspects," *Veh. Syst. Dyn.*, vol. 20, no. 3/4, pp. 121–176, Jan. 1991.
[16] P. W. A. Zegelaar and H. B. Pacejka, "The in-plane dynamics of tyres on uneven roads," *Veh. Syst. Dyn. Suppl.*, vol. 25, pp. 714–730, Jan. 1996.
[17] E. Denti and D. Fanteria, "Models of wheel contact dynamics: An analytical study on the in-plane transient response of a brush model," *Veh. Syst. Dyn.*, vol. 34, no. 3, pp. 199–225, Sep. 2000.
[18] M. Burckhardt, *Fahrwerktechnik: Radschlupfregelsysteme*. Würzburg, Germany: Vogel-Verlag, 1993.
[19] L. Alvarez and J. Yi, "Adaptive emergency braking control in automated highway systems," in *Proc. IEEE Conf. Decision and Control*, Phoenix, AZ, 1999, vol. 4, pp. 3740–3745.
[20] G. Rill, *Simulation von Kraftfahrzeugen*. Wiesbaden, Germany: Vieweg, 1994.
[21] H. B. Pacejka and E. Bakker, "The magic formula tyre model," in *Proc. 1st Int. Colloq. Tyre Models Vehicle Dynamics Analysis*, Delft, The Netherlands, 1991, pp. 1–18.
[22] P. Dahl, "A solid friction model," The Aerospace Corp., El Segundo, CA, Tech. Rep. TOR-0158(3107-18)-1, 1976.
[23] ——, "Measurement of solid friction parameters of ball bearings," in *Proc. 6th Annu. Symp. Incremental Motion, Control Systems and Devices*, Urbana, IL, 1977, pp. 49–60.
[24] P.-A. Bliman and M. Sorine, "Friction modeling by hysteresis operators: Application to Dahl, stiction and Stribeck effects," in *Proc. Conf. 'Models of Hysteresis'*, Trento, Italy, 1991, pp. 10–19.
[25] ——, "A system-theoretic approach of systems with hysteresis: Application to friction modeling and compensation," in *Proc. Eur. Control Conf.*, Groningen, The Netherlands, 1993, pp. 1844–1849.
[26] ——, "Easy-to-use realistic dry friction models for automatic control," in *Proc. Eur. Control Conf.*, Rome, Italy, 1994, pp. 3788–3794.
[27] C. Canudas de Wit, H. Olsson, K. J. Astrom *et al.*, "A new model for control of systems with friction," *IEEE Trans. Autom. Control*, vol. 40, no. 3, pp. 419–425, Mar. 1995.
[28] C. Canudas de Wit and P. Tsiotras, "Dynamic tire friction models for vehicle traction control," in *Proc. IEEE Conf. Decision and Control*, Phoenix, AZ, 1999, vol. 4, pp. 3746–3751.
[29] H. Olsson, "Control systems with friction," Ph.D. thesis, Dept. Automatic Control, Lund Inst. Technology, Lund, Sweden, 1996.
[30] N. Barabanov and R. Ortega, "Necessary and sufficient conditions for passivity of the LuGre friction model," *IEEE Trans. Autom. Control*, vol. 45, no. 4, pp. 830–832, Apr. 2000.

[31] M. Gafvert, "Comparisons of two dynamic friction models," in *Proc. IEEE Int. Conf. Control Applications*, Hartford, CT, 1997, pp. 386–391.

[32] H. Olsson, K. J. Astrom, C. Canudas de Wit *et al.*, "Friction models and friction compensation," *Eur. J. Control*, vol. 4, no. 3, pp. 176–195, Dec. 1998.

[33] J. Deur, "Modeling and analysis of longitudinal tire dynamics based on the LuGre friction model," in *Proc. 3rd Int. Federation Automatic Control (IFAC) Workshop Advances Automotive Control*, Karlsruhe, Germany, 2001, pp. 101–106.

[34] ——, "A brush-type dynamic tire friction model for non-uniform normal pressure distribution," in *Proc. 15th Triennial Int. Federation Automatic Control (IFAC) World Congr.*, Barcelona, Spain, 2002. CD-ROM.

[35] C. Canudas-de-Wit, P. Tsiotras, and E. Velenis, "Dynamic friction models for longitudinal road/tire interaction: Theoretical advances," in *21st IASTED Conf. Modelling, Identification and Control*, Innsbruck, Austria, 2002, pp. 48–53.

[36] ——, "Dynamic friction models for longitudinal road/tire interaction: Experimental results," in *Proc. 21st IASTED Conf. Modelling, Identification and Control*, Innsbruck, Austria, 2002. CD-ROM.

[37] C. Canudas de Wit, P. Tsiotras, E. Velenis *et al.*, "Dynamic friction models for road/tire longitudinal interaction," *Veh. Syst. Dyn.*, vol. 39, no. 3, pp. 189–226, Mar. 2003.

[38] J. Yi, L. Alvarez, X. Claeys *et al.*, "Emergency braking control with an observer-based dynamic tire road friction model and wheel angular velocity measurement," *Veh. Syst. Dyn.*, vol. 39, no. 2, pp. 81–97, Feb. 2003.

[39] M. Segel, "Theoretical prediction and experimental substantiation of the response of the automobile to steering control," in *Proc. Automobile Division Institute Mechanical Engineers*, Hartford, CT, 1956, vol. 7, pp. 310–330.

[40] J. Kasselmann and T. Keranen, "Adaptive steering," *Bendix Tech. J.*, vol. 2, no. 1, pp. 26–35, 1969.

[41] J. Ackermann, "Robust car steering by yaw rate control," in *Proc. 29th IEEE Conf. Decision and Control*, Honolulu, HI, 1990, pp. 2033–2034.

[42] J. Ackermann and W. Dareberg, "Automatic track control of a city bus," *IFAC Theory Report on Benchmark Problems for Control Systems Design*, 1990.

[43] B. Breuer, V. Eichorn, and J. Roth, "Measurement of tyre/road friction ahead of car and inside the tyre," in *Proc. Int. Symp. Advanced Vehicle Control*, Yokohama, Japan, 1992, pp. 347–353.

[44] Q. Qu and Y. Liu, "On lateral dynamics of vehicles based on nonlinear characteristics of tires," *Veh. Syst. Dyn.*, vol. 34, no. 2, pp. 131–141, Aug. 2000.

[45] E. Ono, S. Hosoe, D. Tuan *et al.*, "Bifurcation in vehicle dynamics and robust front wheel steering control," *IEEE Trans. Contr. Syst. Technol.*, vol. 6, no. 3, pp. 412–420, May 1998.

[46] J. Stephant, A. Charara, and D. Meizel, "Virtual sensor: Application to vehicle sideslip angle and transversal forces," *IEEE Trans. Ind. Electron.*, vol. 51, no. 2, pp. 278–289, Apr. 2004.

[47] Y. Furukawa, N. Yuhara, S. Sano *et al.*, "A review of four-wheel steering studies from the viewpoint of vehicle dynamics and control," *Veh. Syst. Dyn.*, vol. 18, no. 2, pp. 151–186, Jun. 1989.

[48] P. Raksincharoensak, M. Nagai, and H. Mouri, "Investigation of automatic path tracking control using four-wheel steering vehicle," in *Proc. IEEE Int. Vehicle Electronics Conf.*, Tottori, Japan, 2001, pp. 73–77.

[49] J. Ackermann and W. Sienel, "Robust yaw damping of cars with front and rear wheel steering," *IEEE Trans. Contr. Syst. Technol.*, vol. 1, no. 1, pp. 15–20, Mar. 1993.

[50] H. Peng and M. Tomizuka, "Lateral control of front-wheel-steering rubber-tire vehicles," Univ. California Press, Berkeley, PATH Research Report UCB-ITS-PRR-90-5, 1990.

[51] T. A. Johansen, I. Petersen, J. Kalkkuhl, and J. Ludemann, "Gain-scheduled wheel slip control in automotive brake systems," *IEEE Trans. Contr. Syst. Technol.*, vol. 11, no. 6, pp. 799–811, Nov. 2003.

[52] J. P. Maurice, M. Berzeri, and H. B. Pacejka, "Pragmatic tyre model for short wavelength side slip variations," *Veh. Syst. Dyn.*, vol. 31, no. 2, pp. 65–94, Feb. 1999.

[53] J. Stephant, A. Charara, and D. Meizel, "Force model comparison on the wheel-ground contact for vehicle dynamics," in *IEEE Intelligent Vehicle Symp.*, Versailles, France, 2002, vol. 2, pp. 589–593.

[54] G. Mastinu and E. A. Pairana, "A semi-analytical tyre model for steady and transient state simulations," in *Proc. 1st Int. Colloq. Tyre Models Vehicle Dynamics Analysis*, Delft, The Netherlands, 1991, pp. 58–81.

[55] H. B. Pacejka and I. Besseling, "Magic formula tyre model with transient properties," in *Proc. 2nd Int. Colloq. Tyre Models Vehicle Dynamics Analysis*, Berlin, Germany, 1997, pp. 234–249.

[56] M. Gafvert and J. Svendenius, "Construction of semi-empirical tire models for combined slip," Dept. Automatic Control, Lund Inst. Technol., Lund, Sweden, Tech. Rep. ISRN LUTFD2/TFRT7606SE, 2003.

[57] J.-O. Hahn, R. Rajamani, and L. Alexander, "GPS-based real-time identification of tire-road friction coefficient," *IEEE Trans. Contr. Syst. Technol.*, vol. 10, no. 3, pp. 331–343, May 2002.

[58] D. J. Schuring, W. Pelz, and M. G. Pottinger, "A model for combined tire cornering and braking forces," *Investigations and Analysis in Vehicle Dynamics and Simulation*, pp. 61–83, 1996, Warrendale, PA: SAE Int. SAE 960180.

[59] G. Gim and P. E. Nikravesh, "An analytical model of pneumatic tyres for vehicle dynamics simulations, part 2: Comprehensive slips," *Int. J. Veh. Des.*, vol. 12, no. 1, pp. 19–39, Jan. 1991.

[60] X. Claeys, J. Yi, L. Alvarez *et al.*, "A dynamic tire/road friction model for 3D vehicle control and simulation," in *Proc. IEEE Intelligent Transportation Systems Conf.*, Oakland, CA, 2001, pp. 483–488.

[61] ——, "Tire friction modeling under wet road conditions," in *Proc. American Control Conf.*, Arlington, VA, 2001, vol. 3, pp. 1794–1799.

[62] E. Velenis, P. Tsiotras, and C. Canudas de Wit, "Extension of the LuGre dynamic tire friction model to 2D motion," in *Proc. 10th Mediterranean Conf. Control and Automation*, Lisbon, Portugal, 2002. CD-ROM.

[63] J. Martinez, J. Avila, and C. Canudas, "A new bicycle vehicle model with dynamic contact friction," in *Proc. 1st Int. Federation Automatic Control (IFAC) Symp. Automotive Control*, Salerno, Italy, 2004. CD-ROM.

[64] T. L. Ford and F. S. Charles, *Heavy Duty Truck Tire Engineering*, 1988. SAE 880001.

[65] E. Gohring, E. C. Von Glasner, and H. C. Pflug, *Contribution to the Force Transmission Behavior of Commercial Vehicle Tires*, 1991. SAE 912692.

[66] M. Gafvert, "Topics in modeling, control, and implementation in automotive systems," Ph.D. dissertation, Dept. Automatic Control, Lund Inst. Technol., Lund, Sweden, 2003. ISSN 0280-5316, ISRN LUTFD2/TFRT-1066-SE.

[67] G. Mavros, H. Rahnejat, and P. King, "Investigation of steady-state tyre force and moment generation under combined longitudinal and lateral slip conditions," *Veh. Syst. Dyn.*, vol. 41, pp. 351–360, Jan. 2004.

[68] A. Lawrence, *Modern Inertial Technology*. New York: Springer-Verlag, 1993.

[69] F. Napolitano, T. Gaiffe, Y. Cottreau *et al.*, "PHINS: The first inertial navigation system based on fiber optic gyroscopes," in *Proc. St. Petersburg Int. Conf. Navigation Systems*, St. Petersburg, Russia, 2002. CD-ROM.

[70] R. Usui and A. Ohno, "Recent progress of fiber optic gyroscope and application at JAE," in *Optical Fiber Sensors Conf. Tech. Dig.*, Portland, OR, 2002, vol. 1, pp. 11–14.

[71] E. Nebot, S. Sukkarieh, and H. Durrant-Whyte, "Inertial navigation aided with GPS information," in *Proc. 4th Annu. Conf. Mechatronics and Machine Vision Practice*, Toowoomba, Qld., Australia, 1997, pp. 169–174.

[72] F. X. Cao, D. K. Yang, A. G. Xu *et al.*, "Low cost SINS/GPS integration for land vehicle navigation," in *Proc. IEEE 5th Int. Conf. Intelligent Transportation Systems*, Singapore, 2002, pp. 910–913.

[73] C.-Y. Chan, "Magnetic sensing as a position reference system for ground vehicle control," *IEEE Trans. Instrum. Meas.*, vol. 51, no. 1, pp. 43–52, Feb. 2002.

[74] J. I. Hernandez and C.-Y. Kuo, "Steering control of automated vehicles using absolute positioning GPS and magnetic markers," *IEEE Trans. Veh. Technol.*, vol. 52, no. 1, pp. 150–161, Jan. 2003.

[75] S. M. Donecker, T. A. Lasky, and B. Ravani, "A mechatronic sensing system for vehicle guidance and control," *IEEE/ASME Trans. Mechatronics*, vol. 8, no. 4, pp. 500–510, Dec. 2003.

[76] W. S. Wijesoma, K. R. S. Kodagoda, A. P. Balasuriya *et al.*, "Road edge and lane boundary detection using laser and vision," in *Proc. IEEE/RSJ Int. Conf. Intelligent Robots and Systems*, Maui, HI, 2001, vol. 3, pp. 1440–1445.

[77] U. Eichhorn and J. Roth, "Prediction and monitoring of tyre/road friction," in *XXIV FISITA Congr.*, London, U.K., 1992, pp. 67–74.

[78] B. Breuer, U. Eichhorn, and J. Roth, "Measurement of tyre/road friction ahead of the car and inside the tyre," in *Proc. Int. Symp. Advanced Vehicle Control*, Yokohama, Japan, 1992, pp. 347–353.

[79] S. Germann, M. Wurtenberger, and A. Daiss, "Monitoring of the friction coefficient between tyre and road surface," in *Proc. 3rd IEEE Conf. Control Applications*, Glasgow, U.K., 1994, vol. 1, pp. 613–618.

[80] C. Liu and H. Peng, "Road friction coefficient estimation for vehicle path prediction," *Veh. Syst. Dyn.*, vol. 25, pp. 413–425, Jan. 1996. Supplement.

[81] F. Gustafsson, "Slip-based tire-road friction estimation," *Automatica*, vol. 33, no. 6, pp. 1087–1099, Jun. 1997.

[82] ——, "Monitoring tire-road friction using the wheel slip," *IEEE Control Syst. Mag.*, vol. 18, no. 4, pp. 42–49, Aug. 1998.
[83] S. Muller, M. Uchanski, and K. Hedrick, "Estimation of the maximum tire-road friction coefficient," *ASME J. Dyn. Syst. Meas. Control*, vol. 125, no. 4, pp. 607–617, Dec. 2003.
[84] U. Kiencke and A. Daiss, "Estimation of tyre friction for enhanced ABS systems," in *Proc. Int. Symp. Advanced Vehicle Control*, Tsukuba City, Japan, 1994. CD-ROM.
[85] W. Hwang and B.-S. Song, "Road condition monitoring system using tire-road friction estimation," in *Proc. Int. Symp. Advanced Vehicle Control*, Ann Arbor, MI, 2000, pp. 437–442.
[86] J. Wang, L. Alexander, and R. Rajamani, "Friction estimation on highway vehicles using longitudinal measurements," *ASME J. Dyn. Syst. Meas. Control*, vol. 126, no. 2, pp. 265–275, Jun. 2004.
[87] H. Nishira, T. Kawabe, and S. Shin, "Road friction estimation using adaptive observer with periodical σ-modification," in *Proc. IEEE Int. Conf. Control Applications*, Kohala Coast, HI, 1999, vol. 1, pp. 662–667.
[88] K. Yi, K. Hedrick, and S. C. Lee, "Estimation of tire-road friction using observer based identifiers," *Veh. Syst. Dyn.*, vol. 31, no. 4, pp. 233–261, Apr. 1999.
[89] C. Canudas de Wit and R. Horowitz, "Observers for tire/road contact friction using only wheel angular velocity information," in *Proc. IEEE Conf. Decision and Control*, Phoenix, AZ, 1999, vol. 4, pp. 3932–3937.
[90] J. Yi, L. Alvarez, R. Horowitz *et al.*, "Adaptive emergency braking control using a dynamic tire/road friction model," in *Proc. IEEE Conf. Decision and Control*, Sydney, Australia, 2000, vol. 1, pp. 456–461.
[91] J. Yi, L. Alvarez, X. Claeys *et al.*, "Emergency braking control with an observer-based dynamic tire/road friction model and wheel angular velocity information," in *Proc. American Control Conf.*, Arlington, VA, 2001, vol. 1, pp. 19–24.
[92] L. Li, F.-Y. Wang, G. Shan *et al.*, "Design of tire fault observer based on estimation of tire/road friction conditions," *Automatica Sinica*, vol. 28, no. 5, pp. 689–694, Oct. 2003.
[93] J. R. Zhang, S. J. Xu, and A. Rachid, "Robust sliding mode observer for automatic steering of vehicles," in *Proc. IEEE Intelligent Transportation Systems*, Dearborn, MI, 2000, pp. 89–94.
[94] C. Lee, K. Hedrick, and K. Yi, "Real-time slip-based estimation of maximum tire-road friction coefficient," *IEEE/ASME Trans. Mechatronics*, vol. 9, no. 2, pp. 454–458, Jun. 2004.
[95] D. M. Bevly, J. C. Gerdes, and C. Wilson, "The use of GPS based velocity measurements for measurement of sideslip and wheel slip," *Veh. Syst. Dyn.*, vol. 38, no. 2, pp. 127–147, Feb. 2002.
[96] R. Daily and D. M. Bevly, "The use of GPS for vehicle stability control systems," *IEEE Trans. Ind. Electron.*, vol. 51, no. 2, pp. 270–277, Apr. 2004.
[97] W. Sienel, "Estimation of the tire cornering stiffness and its application to active car steering," in *Proc. IEEE Conf. Decision and Control*, San Diego, CA, 1997, vol. 5, pp. 4744–4749.
[98] S. Saraf and M. Tomizuka, "Slip angle estimation for vehicles on automated highways," in *Proc. American Control Conf.*, Albuquerque, NM, 1997, vol. 3, pp. 1588–1592.
[99] L. R. Ray, "Nonlinear tire force estimation and road friction identification: Simulation and experiments," *Automatica*, vol. 33, no. 10, pp. 1819–1833, Oct. 1997.
[100] ——, "Experimental determination of tire forces and road friction," in *Proc. American Control Conf.*, Philadelphia, PA, 1998, vol. 3, pp. 1843–1847.
[101] B. Samadi, R. Kazemi, K. Y. Nikravesh *et al.*, "Real-time estimation of vehicle state and tire-road friction forces," in *Proc. American Control Conf.*, Arlington, VA, 2001, vol. 5, pp. 3318–3323.
[102] K. Huh, J. Kim, K. Yi *et al.*, "Monitoring system design for estimating the lateral tire force," in *Proc. American Control Conf.*, Anchorage, AK, 2002, vol. 2, pp. 875–880.
[103] S. Kimbrough, "A brake control strategy for emergency stops that involve steering: Part 1 theory," in *Proc. 2nd Symp. Transportation Systems, ASME Winter Annu. Meeting*, Dallas, TX, 1990. CD-ROM.
[104] ——, "A brake control strategy for emergency stops that involve steering: Part 2 implementation issues and simulation results," in *Proc. 2nd Symp. Transportation Systems, ASME Winter Annu. Meeting*, Dallas, TX, 1990. CD-ROM.
[105] R. Emig, H. Goebels, and H. J. Schramm, "Antilock braking systems (ABS) for commercial vehicles—Status 1990 and future prospects," in *Vehicle Electronics 90's: Proc. Int. Congr. Transportation Electronics*, 1990, pp. 515–523.
[106] R. Bosch, *Automotive Handbook*, 4th ed. Cambridge, MA: Robert Bentley Publisher, 1997.
[107] M. Schinkel and K. Hunt, "Anti-lock braking control using a sliding mode like approach," in *Proc. American Control Conf.*, Anchorage, AK, 2002, vol. 3, pp. 2386–2391.
[108] P. E. Wellstead and N. B. O. L. Pettit, "Analysis and redesign of an antilock brake system controller," *Proc. Inst. Elect. Eng.—Control Theory Appl.*, vol. 144, no. 5, pp. 413–426, Sep. 1997.
[109] P. Tsiotras and C. Canudas-de-Wit, "On the optimal braking of wheeled vehicles," in *Proc. American Control Conf.*, Chicago, IL, 2000, vol. 1, pp. 569–573. no. 6.
[110] D. Zhang, H. Zheng, J. Sun *et al.*, "Simulation study for anti-lock braking system of a light bus," in *Proc. IEEE Int. Vehicle Electronics Conf.*, Changchun, China, 1999, pp. 70–77.
[111] S. Drakunov, U. Ozguner, P. Dix *et al.*, "ABS control using optimum search via sliding modes," *IEEE Trans. Contr. Syst. Technol.*, vol. 3, no. 1, pp. 79–85, Mar. 1995.
[112] M. Krstik and H.-H. Wang, "Design and stability analysis of extremum seeking feedback for general nonlinear systems," in *Proc. IEEE Conf. Decision and Control*, San Diego, CA, 1997, pp. 1743–1748.
[113] I. Petersen, T. A. Johansen, J. Kalkkuhl *et al.*, "Wheel slip control using gain-scheduled LQ-LPV/LMI analysis and experimental results," in *Proc. Eur. Control Conf.*, Cambridge, U.K., 2003. CD-ROM.
[114] S. Taheri and E. H. Law, "Slip control braking of an automobile during combined braking and steering maneuvers," in *ASME Design Engineering Division (Publication) DE*, vol. 40. Dearborn, MI: Ford Motor Co., 1991, pp. 209–227.
[115] K. Yi, K. Hedrick, and S. Lee, "Estimation of tire-road friction using observer based identifiers," *Veh. Syst. Dyn.*, vol. 31, no. 4, pp. 233–261, Apr. 1999.
[116] T. Shim and D. Margolis, "Model-based road friction estimation," *Veh. Syst. Dyn.*, vol. 41, no. 4, pp. 249–276, Apr. 2004.
[117] W. R. Pasterkamp and H. B. Pacejka, *Application of Neural Networks in the Estimation of Tire/Road Friction Using the Tire as a Sensor*, 1997. SAE 971122.
[118] M. Beato, V. Ciaravola, M. Russo *et al.*, "Lateral tyre force by a Milliken test on a flat track roadway simulator," *Veh. Syst. Dyn.*, vol. 34, no. 2, pp. 117–129, Aug. 2000.
[119] J. A. Cabrera, A. Ortiz, E. Carabias *et al.*, "An alternative method to determine the magic tyre model parameters using genetic algorithms," *Veh. Syst. Dyn.*, vol. 41, no. 2, pp. 109–127, Feb. 2004.
[120] H. S. Bae, J. Ryu, and J. C. Gerdes, "Road grade and vehicle parameter estimation for longitudinal control using GPS," in *Proc. IEEE Conf. Intelligent Transportation Systems*, Oakland, CA, 2001, pp. 166–171.
[121] W. R. Patserkamp and H. B. Pacejka, "The tire as a sensor to estimate friction," *Veh. Syst. Dyn.*, vol. 27, no. 5/6, pp. 409–422, Jun. 1997.
[122] A. Pohl, R. Steindl, and L. Reindl, "The 'intelligent tire' utilizing passive SAW sensors measurement of tire friction," *IEEE Trans. Instrum. Meas.*, vol. 48, no. 6, pp. 1041–1046, Dec. 1999.
[123] A. Pohl, "A review of wireless SAW sensors," *IEEE Trans. Ultrason., Ferroelectr., Freq. Control*, vol. 47, no. 2, pp. 317–332, Mar. 2000.
[124] M. Mizuno, H. Sakai, K. Oyama *et al.*, "The development of the tire side force model considering the dependence of surface temperature of tire," *Veh. Syst. Dyn. Suppl.*, vol. 41, pp. 361–370, 2004.
[125] F.-Y. Wang, P. B. Mirchandani, and Z. Wang, "The VISTA project and its applications," *IEEE Intell. Syst.*, vol. 17, no. 6, pp. 72–75, Nov./Dec. 2002.
[126] F.-Y. Wang, X. Wang, L. Li *et al.*, "Creating a digital-vehicle proving ground," *IEEE Intell. Syst.*, vol. 18, no. 2, pp. 12–15, Mar.–Apr. 2003.
[127] N.-N. Zheng, S. Tang, H. Cheng *et al.*, "Toward intelligent driver-assistance and safety warning system," *IEEE Intell. Syst.*, vol. 19, no. 2, pp. 8–11, Mar./Apr. 2004.

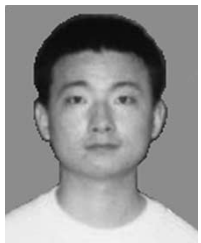

Li Li (S'05–M'06) received the B.S. degree in electronics and information engineering from Huazhong University of Science and Technology, Wuhan, China, in 1999, and the M.S. degree in industrial engineering in 2003 and the Ph.D. degree in systems engineering in 2005, both from the University of Arizona, Tucson.

He is currently an Adjunct Assistant Professor with the Department of Systems and Industrial Engineering, University of Arizona, working in the fields of intelligence and optimization, control and sensory, intelligent vehicles, and intelligent transportation systems.

Fei-Yue Wang (S'87–M'89–SM'94–F'03) received the B.S. degree in chemical engineering from Qingdao University of Science and Technology, Qingdao, China, the M.S. degree in mechanics from Zhejiang University, Hangzhou, China, and the Ph.D. degree in electrical, computer, and systems engineering from the Rensselaer Polytechnic Institute, Troy, New York, in 1982, 1984, and 1990, respectively.

He joined the University of Arizona in 1990 and became a Full Professor of Systems and Industrial Engineering in 1999 and currently is the Director of the Program in Advanced Research for Complex Systems. In 1999, he found the Intelligent Control and Systems Engineering Center at the Institute of Automation, Chinese Academy of Sciences, Beijing, China, under the support of the Outstanding Overseas Chinese Talents Program. Since 2002, he has been the Director of the Key Laboratory of Complex Systems and Intelligence Science at the Chinese Academy of Sciences. His current research interests include modeling, analysis, and control mechanism of complex systems; agent-based control systems; intelligent control systems; real-time embedded systems and application-specific operating systems (ASOS); applications in intelligent transportation systems, intelligent vehicles (IVs) and telematics, web caching and service caching, smart appliances and home systems, and network-based automation systems. He has published more than 200 books, book chapters, and papers in those areas since 1984 and received more than $20M USD and over ¥50M RMB from the National Science Foundation (NSF), Department of Energy (DOE), Department of Transportation (DOT), National Natural Science Foundation (NNSF), Chinese Academy of Sciences (CAS), Ministry of Science and Technology (MOST) China, Caterpillar, International Business Machines (IBM), Hewlett-Packard (HP), American Telephone and Telegraph Corporation (AT&T), General Motors (GM), BHP Billiton (BHP), Acuity CiMatrix, ABB Group (ABB), and Kelon.

Dr. Wang received the Caterpillar Research Invention Award with Dr. P. J. A. Lever in 1996 for his work in robotic excavation, and the National Outstanding Young Scientist Research Award from the NNSF of China in 2001, as well as various industrial awards for his applied research from major corporations. He was the Editor-in-Chief of the International Journal of Intelligent Control and Systems from 1995 to 2000, Editor-in-Charge of Series in Intelligent Control and Intelligent Automation from 1996 to 2004, and currently is the Editor-in-Charge of Series in Complex Systems and Intelligence Science. He is also the Associated Editor and the Editor for the Intelligent Transportation Systems Department of the IEEE Intelligent Systems, and an Associate Editor of the IEEE TRANSACTIONS ON SYSTEMS, MAN, AND CYBERNETICS, IEEE TRANSACTIONS ON ROBOTICS AND AUTOMATION, IEEE TRANSACTIONS ON INTELLIGENT TRANSPORTATION SYSTEMS, and several other international journals. He is an elected member of the IEEE SMC Board of Governors and the AdCom of the IEEE Nanotechnology Council, the President-Elect of IEEE Intelligent Transportation Systems Society, and Chair of the Technical Committee on System Complexity of the Chinese Association of Automation. He was the Program Chair of the 1998 IEEE Int'l Symposium on Intelligent Control, the 2001 IEEE Int'l Conference on Systems, Man, and Cybernetics, the Chair for Workshops and Tutorials for the 2002 IEEE Int'l Conf. on Decision and Control (CDC), the General Chair of the 2003 IEEE Int'l Conference on Intelligent Transportation Systems, Co-Program Chair of the 2004 IEEE Int'l. Symposium on Intelligent Vehicles, and will be the General Chair for the same conference in 2005. He is also the General Chair of the IEEE 2005 International Conference on Networking, Sensing, and Control. He was the Vice President and one of the major contributors of the American Zhu Kezhen Education Foundation, and a member of the Boards of Directors of five companies in information technology and automation. He is also a member of Sigma Xi, Association for Computing Machinery (ACM), American Society of Mechanical Engineers (ASME), American Society for Engineering Education (ASEE), and International Council of Systems Engineering (INCOSE).

Qunzhi Zhou received the B.S. degree in automation engineering from Tsinghua University, Beijing, China, in 2001, and the M.S. degree in control engineering from the Institute of Automation, Chinese Academy of Science, Beijing, China, in 2004.

He is currently working in fields of intelligent control and intelligent vehicles (IVs).